Alberta Glacier Inventory and Ice Volume Estimation

Prepared by Shawn Marshall and Eric White
Crowfoot Ice Research and Consulting
8-205 Carey, Canmore, AB, T1W 2R7

December 2010

Haig Glacier, Peter Lougheed Provincial Park, Kananaskis   September 11, 2009

Contents

Executive Summary

This report assesses the area and volume of the glacier water resources in the glaciated river basins of Alberta: the Bow, Red Deer, North Saskatchewan, Athabasca, and Peace. Runoff in the Peace River Basin includes eastward-routed meltwater from glaciers in the northern Rockies of British Columbia (B.C.), and we include these glaciers in the analysis.

Maps of glacier area in western Canada have recently been generated by the Western Canadian Cryospheric Network (WC²N) for 1985 and 2005, providing the first complete inventory of glacier cover in Alberta and B.C. Western Canada lost about 11% of its glacier area over this period, with area loss exceeding 20% on the eastern slopes of the Canadian Rockies. Glacier area is difficult to relate to glacier volume, which is the attribute of relevance to water resources. We apply several possible volume-area scaling relationships and glacier slope-thickness relationships to estimate the volume of glacier ice in the headwaters regions of rivers that spring from the eastern slopes of the Rockies. The mean estimate for ice volume on the eastern slopes is 55 ± 15 km³, with 47 ± 13 km³ residing in Alberta (Table E1). The uncertainty is high because there is a paucity of glacier-thickness data in the Rockies. We cannot preclude higher values because the data that is available indicates that large valley glaciers in the Rocky Mountains may be anomalously thick, relative to what is typical in the global database that forms the basis for empirical volume-area scaling relationships.

Table E1. Glacier count, area and volume estimates for Alberta river basins, based on the WC²N glacier inventory for 2005. Best estimates are based on the mean prediction from four different methods for ice volume estimation.

Basin	Count	Area (km²)	Glacier Volume (km³)	
			Range	Best estimate
Bow	96	60.1	2.1-3.6	3.0 ± 0.7
Red Deer	22	16.6	0.6-1.0	0.9 ± 0.2
North Saskatchewan	258	286.3	13-19	17.5 ± 4.4
Athabasca	271	320.5	12-18	16.7 ± 4.2
Peace(AB)	94	107.6	6-14	8.8 ± 1.4
Peace(AB and BC)	363	276.7	13-23	16.9 ± 4.2
Alberta	741	791.1	35-55	47 ± 13
Eastern slopes	1010	960.3	43-67	55 ± 15

Incorporating multivariate statistical analysis using observed mass balance data from Peyto Glacier, Alberta and synoptic meteorological conditions in the Canadian Rockies (1966-2007), we develop a regional glacier mass balance model for the eastern slopes of the Rockies. The mass balance model is constrained by available observations from two other sites in the Rockies, Haig and Kwadacha Glaciers. This model provides an estimate of recent (2000-2007) glacier volume losses on the eastern slopes, 0.62 ± 0.09 km³yr⁻¹ (a decline of 1.1% yr⁻¹). Volume losses are also analyzed for each basin, providing an

estimate of recent glacier contributions to streamflow in different catchments. Ice volume losses from the eastern slopes from 2000-2007 represented 3-4% of mean annual discharge and 7-8% of late summer (July to September) runoff in the North Saskatchewan and Bow Rivers in Edmonton and Calgary, respectively (Table E2).

Table E2. Average annual discharge, estimated naturalized July to September discharge, and estimated contributions from glacier volume loss (water equivalent) at sites of interest in each major glacier-fed Alberta river basin, 2000-2007. *N* and *f* indicate the number of Water Survey of Canada sites used to reconstruct the naturalized flows and the percentage of annual yield represented by these upstream sites.

Basin	Site	N	f (%)	Average yield (km^3) Q_a	Q_{JAS}	Q_g	% glacial *ann*	*JAS*
Bow	Calgary	2	45.4	2.6	1.1	0.074	2.8	6.7
Red Deer	Red Deer	3	62.2	1.4	0.5	0.009	0.6	1.8
N. Sask.	Edmonton	5	51.9	5.6	2.8	0.206	3.7	7.4
Athabasca	Ft. McMurray	1	100.0	15.9	6.6	0.134	0.8	2.0
Peace	Peace River	15	74.2	59.7	18.2	0.142	0.2	0.8

We restrict our attention to runoff associated with glacier retreat: tapping of the water that is stored as ice in the glaciers of the Rocky Mountains. Runoff from the seasonal snowpack on glaciers is presumably 'renewable' – it will continue to feed the rivers even if the glaciers disappear from the landscape. With loss of glacier ice, however, this snowpack contribution may also decline, as glaciers act as snow traps that encourage snow accumulation. The cold environment on glaciers also preserves much of this snow until later in the summer melt season, while routing through the glacier can introduce delays of weeks to months in delivering meltwater to the rivers, particularly in the early summer. Glacier retreat is therefore expected to result in earlier melting and runoff of seasonal snow from sites that are presently glaciated. We do not explore the expected changes to the seasonal snowpack or hydrological routing here, but this warrants further study.

The final section of this study examines future volume changes for the glaciers of the Rockies, using the regional mass balance model, future climate scenarios for the Rockies, and a simple model of glacier dynamics that describes the evolution of glacier geometry and the mass balance feedbacks associated with glacier retreat. Our projections indicate that glaciers on the eastern slopes will lose about 40% of their volume by 2100 if climate stabilizes near its current state, and 80-90% of their volume by 2100 under more realistic scenarios for future climate change. In this situation glacier contributions to streamflow in Alberta are projected to decline from 1.1 km^3 a^{-1} in the early 2000s to 0.1 km^3 a^{-1} by the end of the century.

A manuscript based on our main methods and results has been peer-reviewed and is currently in press in the *Canadian Water Resources Journal*. The following report provides further detail.

1. Introduction

The icefields and mountain glaciers of Alberta are situated on the continental divide and the eastern slopes of the Canadian Rocky Mountains. Alberta's glaciers are concentrated here for two primary reasons: (i) they form at the highest elevations, where temperatures are coolest, and (ii) the continental divide and adjacent slopes receive large amounts of moisture from the Pacific air masses that flow in from B.C. Approximately 37 peaks rise above 3400 m along the spine of the Rockies, making this the highest obstacle that Pacific air masses encounter as they traverse southwestern Canada. Orographic uplift on the western slopes cools the air and induces precipitation. The resultant air masses are largely wrung out as they carry on eastward over the Canadian prairies.

The precipitation gradient in the eastern slopes of the Canadian Rocky Mountains is dramatic. Annual precipitation at the continental divide on Haig Glacier averaged 1900 mm a^{-1} between 2002-2009, for example (unpublished data), compared with 430 mm a^{-1} over this period in Calgary, Alberta (Environment Canada, 2010), which lies 100 km to the east (Figure 1). Most of this falls as snow in the mountains, creating the numerous glaciers and icefields which are one of the hallmarks of the Canadian Rockies.

These glaciers act as natural reservoirs, with snow and ice melt contributing significantly to summer flow in some of Alberta's major rivers: the Bow, Red Deer, North Saskatchewan, Athabasca, and Peace. Glaciers in northeastern B.C. also contribute to the headwaters of the Peace River. Section 2 describes the general glaciological, climatic and hydrological regime of Alberta's glaciers. Section 3 presents an inventory of Alberta's glaciers and their topographic setting. Section 4 provides the first assessment of glacier volume in the province. Section 5 then explores glacier mass balance characteristics and trends in the Rockies, with a preliminary forecast for 21st century glacier changes and the implications for glacier contributions to the major rivers that spring from the Canadian Rockies.

This report draws from several sources, with field sites indicated in Figure 1:

(i)   The published literature, primarily from studies on the Peyto and Athabasca Glaciers, along Alberta's Icefields Parkway.

(ii) Published and unpublished data from University of Calgary fieldwork at three field sites in the Canadian Rockies: the Haig Glacier, Kananaskis (2000-2010), Opabin Glacier, Yoho National Park, B.C. (2005-2008), and Kwadacha Glacier, Lloyd George Icefield, northern B.C. (2007-2010).

(iii) Data and analysis of the Western Canadian Cryospheric Network (WC2N), a research network headed by Brian Menounos at UNBC and funded by the Canadian Network for Climate and Atmospheric Sciences (2006-2010).
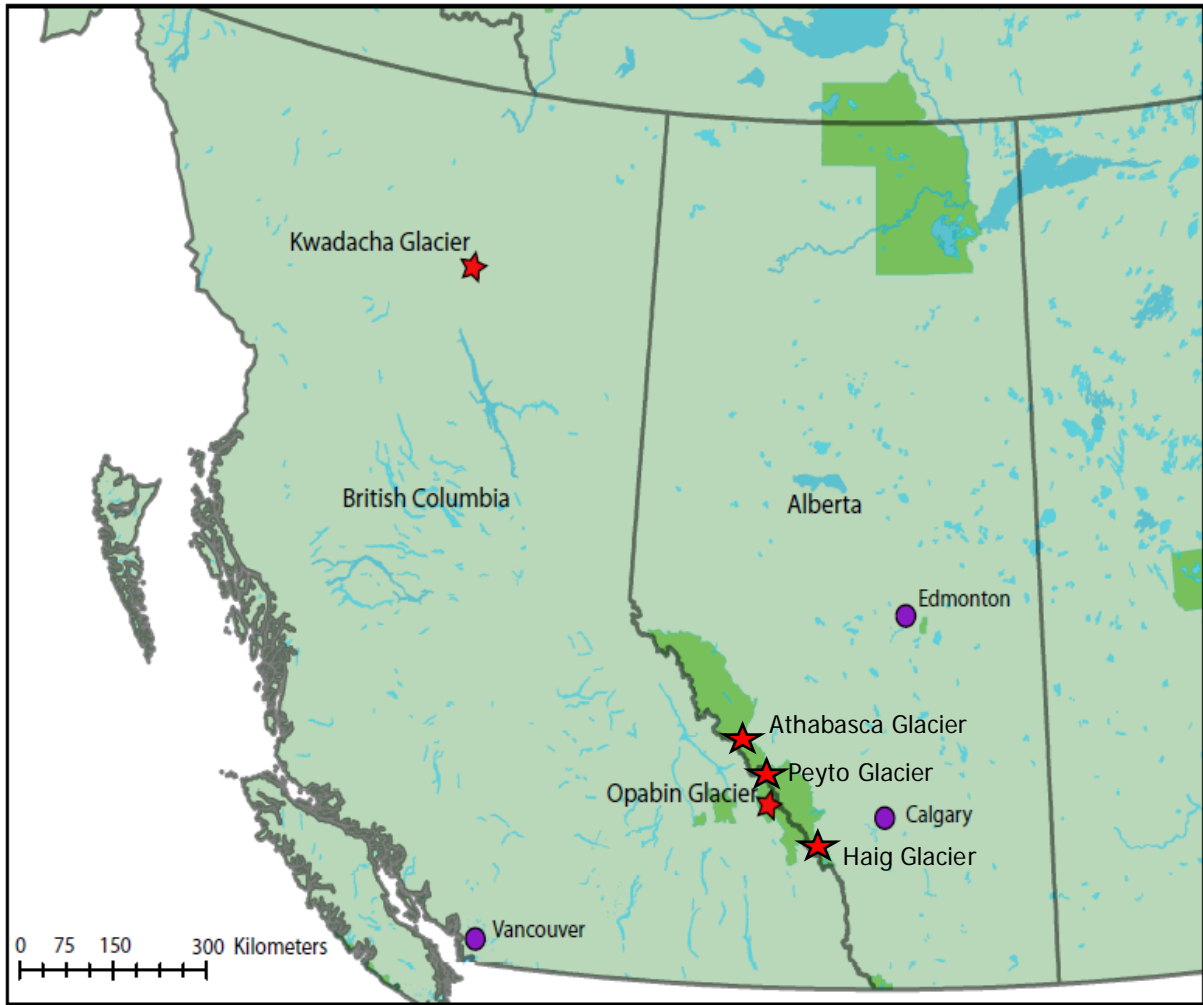
Figure 1. Locations of the glaciers referred to in the report: the Haig Glacier, Kananaskis (50°43' N, 115°18' W), Opabin Glacier, Yoho National Park (51°20' N, 116°18' W), Peyto Glacier, Banff National Park (51°41' N, 116°32' W), Athabasca Glacier, Jasper National Park (52°11' N, 117°16' W), and Kwadacha Glacier, Northern Rockies, B.C. (57°49' N, 124°55' W). These glaciers feed the Kananaskis (Bow), Kicking Horse (Columbia), Mistaya (North Saskatchewan), Athabasca, and Kwadacha (Peace) Rivers, respectively.
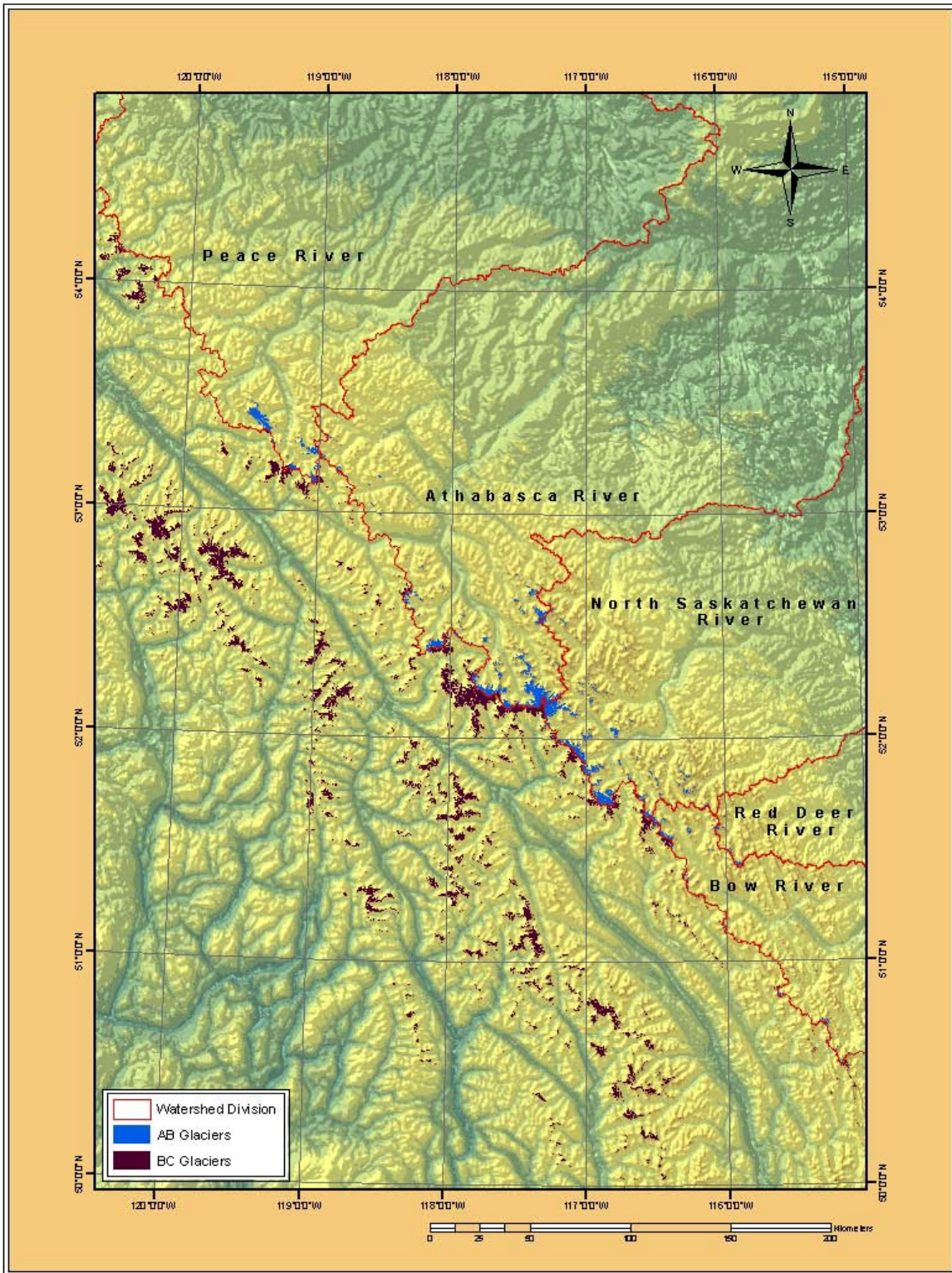
Figure 2. Watershed map depicting Alberta glacier cover and the major river basins analyzed in this report: the Bow, Red Deer, North Saskatchewan, Athabasca, and Peace. Portions of the Peace River catchment extending into B.C. are shown in Figure 3.
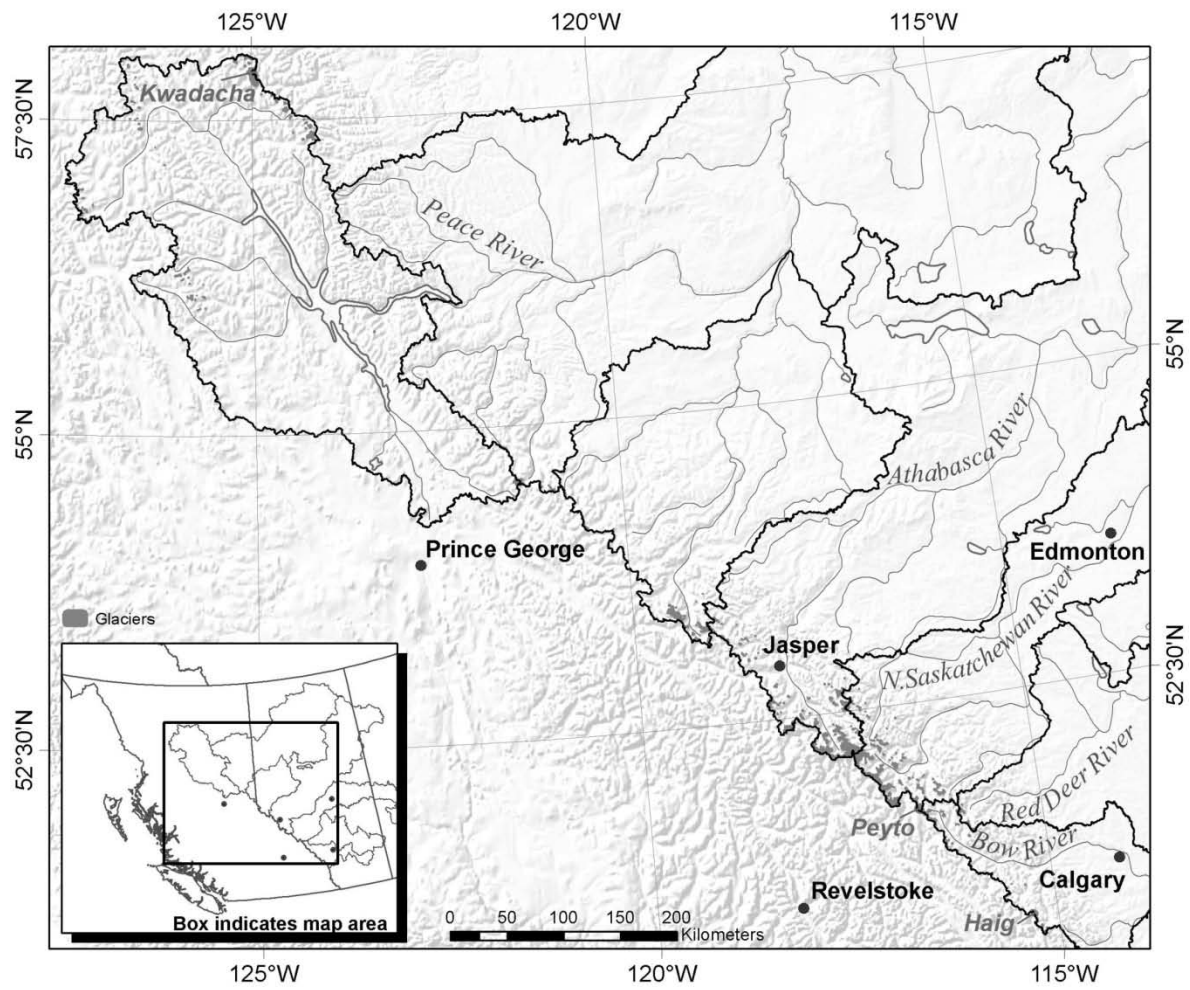
Figure 3. Watersheds draining the eastern slopes of the Canadian Rocky Mountains.

2. Glaciers, Climate, and Hydrology of the Canadian Rockies

2.1 Overview of Rockies Glaciology and Climatology

Glaciers are perennial ice masses that are large enough to experience flow. Gravitationally-driven ice motion occurs through three different mechanisms: internal 'creep' deformation, sliding along the ice-bed interface, and deformation of subglacial sediments. All three processes are believed to be active in the Canadian Rockies, though there are few studies of glacier dynamics in the Rockies. Where they have been measured, typical flow rates are on the order of 10s of metres per year (e.g., ca. 30 m yr^{-1} near the snow-coach turnaround on the Athabasca Glacier; Paterson, 1964). Small cirque glaciers will move at just a few m yr^{-1}.

There is good information about the number and area of glaciers in the Rockies (Section 3), but little is known about ice thickness or volume. Ice thickness estimates require time- and labour-intensive ice radar surveys, executed through towing of an ice radar or low-frequency ground-penetrating radar (GPR) system along the glacier surface or airborne radar surveys. Electromagnetic wave frequencies of 5 to 50 MHz are typically used for glacier depth sounding, as these relatively low frequencies limit signal attenuation and allow penetration of radar pulses through a few 100 m of glacier ice. Resolution at these frequencies is limited; it is of the same order as the wavelength, e.g., 6-60 m for the range of frequencies from 50 to 5 MHz. The antennae in such systems are also cumbersome, with lengths similar to the wavelength, so it is difficult to sled these systems across a glacier. It is customary to set up a survey grid over a glacier, and several km of line can be mapped in a typical day. The ice-bed interface provides a strong electrical contrast, so these systems have good success in mapping subglacial topography and ice thickness.

Other geophysical techniques (e.g., seismic and gravity surveys) have also been applied to ice-thickness mapping, but radar sounding is the prevailing technique. To our knowledge, ice thickness has only been mapped for three glaciers in the Canadian Rockies: the Athabasca, Peyto, and Haig Glaciers. We discuss this data in Section 4.2.

2.1.1 Temperatures in the Canadian Rockies

Glaciers of the Rockies are 'isothermal' – they are at the melting point throughout their depth. This means that free water and ice co-exist englacially and subglacially throughout the year. Near the glacier surface, where the glacier is exposed to the atmosphere, winter cooling freezes the surface seasonally. Because seasonal snow insulates the glacier ice, the depth of the seasonal freezing layer is limited to the seasonal snowpack and the upper few metres of the glacier. Prior to the onset of spring melt, the snowpack typically has a temperature of ca. −5°C. During the spring thaw, percolation of meltwater into the snowpack and release of latent heat from refreezing rapidly restores snowpack temperatures to 0°C each April or May.

There is no simple 'threshold temperature' for a glacier to be viable. A mean annual temperature below 0°C is not a necessary or sufficient condition for glacier ice to exist.

Tidewater glaciers in coastal B.C. and Alaska are vivid examples of this. Because ice flow delivers large fluxes of ice to low elevations, glaciers extend to sea-level environments where mean annual temperatures are several degrees above 0°C. This is intrinsic to all glaciers; glacier ice in the ablation area does not grow *in situ*, but is a consequence of ice transport from the accumulation area to the ablation area.

The mean annual temperature at the terminus of the Haig Glacier (2460 m elevation), the only glacier site in the Rockies where detailed data is available, is approximately −2.1°C (2001-2009). The head of the glacier (2735 m on the continental divide) had a mean temperature of −3.9°C over this period. There is cooling with latitude in the Canadian Rockies, leading to a general pattern of lower elevations for glacier termini in central and northern Alberta. Environment Canada's Sunwapta station on the Icefields Parkway (1555 m) is no longer active, but from 1979-2000 it recorded a mean annual temperature of −0.3°C. This is the most proximal data to the Columbia Icefield, the most glaciated region of Alberta. Terminus elevations of the Columbia's major outlets (e.g., Saskatchewan, Athabasca) are ca. 2100 m; given typical surface-temperature lapse rates of −5.5°C/km in the Rockies (Shea et al., 2004), mean annual temperatures for these outlet glaciers will be close to −3°C. These glaciers descend to lower elevations than those in Kananaskis Country because they are fed by large fluxes of ice from the interior accumulation region of the Columbia Icefield. At the elevation of the Columbia Icefield accumulation area, above ca. 2800 m, mean annual temperatures are estimated to be below −6°C.

2.1.2 Glacier Mass Balance

Glacier mass balance refers to the change in mass of a glacier over a specific time frame, typically one year. Glaciers of the Rockies typically accumulate snow from mid-September through mid-May (the 'accumulation season') and experience melting and runoff from mid-May through mid-September (the 'melt season'). The 'glaciological year' runs from the start of the accumulation season to the end of the subsequent melt season. Net accumulation minus net ablation of snow and ice over this period determines the annual gain or loss of ice from the glacier. This can be expressed as a total balance (kg yr^{-1} or m^3 yr^{-1} water-equivalent (w.e.) for the entire glacier) or a specific balance, per unit-area of the glacier (kg m^{-2} yr^{-1} or m w.e. yr^{-1}). The latter is most commonly employed as it is most intuitive. For example, a specific mass balance of −1 m w.e. yr^{-1} indicates an average glacier-wide thinning of 1 m w.e. for the glaciological year (about 1.1 m of ice). A mass balance of 0 indicates a state of balance (glacier-averaged accumulation equal to melt).

Mass balance can be estimated through remote sensing techniques such as repeat airborne or satellite laser altimetry, which can measure changes in surface elevation. This is difficult to relate to mass changes over snow cover, as snow density is unknown. Repeat altimetry studies have not been done in the Rockies, as LIDAR systems and flight time are costly. Pilot studies on the Peyto and Opabin Glaciers indicate that this is a promising technique for constructing detailed and accurate surface topography, but airborne laser profiling is not yet being conducted operationally for mass balance studies. Available data therefore comes from a small number of field studies carried out by government organizations and university researchers. Field techniques involve late-spring snow surveys to quantify

winter accumulation along with networks of ablation stakes to measure summer melt. The Peyto Glacier has the longest-running mass balance record in the Rockies, 1966 to present. Limited amounts of data are also available from Ram, Haig, and Kwadacha Glaciers. We discuss these mass balance records further in Section 5.

2.2 Overview of Glacier Hydrology

Glaciers act as natural reservoirs for snow, ice, and meltwater. On seasonal time scales, ice melt and temporary meltwater storage within a glacier lead to large amounts of late-summer discharge. In many alpine streams this is the sole source of baseflow in late summer and early fall, after the seasonal snowpack has melted away. On decadal to centennial time scales, mountain glaciers advance and retreat over the landscape, giving long-term storage and release of water. The next subsection describes the general character of glacier hydrology, followed by an extended discussion of the ways in which glacier cover affect regional hydrology.

2.2.1 Glacier hydrology

The glacier surface consists of seasonal snow, multiyear firn, and glacial ice. Firn is present in the upper accumulation area, where it can be 10s of metres thick. In theory, firn can be found everywhere above the glacier's equilibrium line altitude (ELA), increasing in thickness with altitude. During negative mass-balance years, however, firn ablates above the ELA. A sequence of negative mass-balance years can remove much of the firn, and 20th-century warming has caused many small alpine glaciers to lose their firn layers entirely (e.g., Paul et al., 2004). In this case, glacial ice underlies seasonal snow cover over the entire surface area of the glacier. This difference is significant for the flow and storage of water in the upper few metres of the glacier surface.

On a glacier surface, meltwater channels carve into the ice and wind sinuously downslope, sometimes pouring off the front of the glacier and sometimes plunging into deep moulins and crevasses. Water that disappears into the glacier may be stored internally or transported through a drainage network within the glacier. In the latter case it typically descends to the glacier bed to join the subglacial drainage system. At the glacier front, the water usually emerges as a few major streams flowing out of tunnels.

Most of the water in mountain glaciers is produced from melting at the glacier surface. Englacial and basal melting also contribute to the water budget, while rainfall and groundwater provide additional, external sources of water to a glacier. Exchanges between the groundwater and the subglacial drainage system can be two-way (Flowers et al., 2005), but these are seldom measured and are not well-understood.

Early in the melt season, glacier hydrology is not significantly different from that of seasonal snow in nonglacial environments. Surface meltwater percolates and refreezes until the snowpack becomes saturated and isothermal (reaches 0°C throughout), at which point runoff begins. There are two major differences between non-glacial and glacial snowpacks, both involving the underlying surface. First, the underlying firn or ice never has a temperature exceeding the melting point, and this limits how much heat can flow up into the snowpack; there is no geothermal heat flux into the seasonal snowpack. The

second difference is the presence of an impermeable ice surface where glacier ice underlies the seasonal snowpack, a situation analogous to snowpacks on landscapes of bare bedrock or permafrost. Meltwater that drains to the snow-ice interface ponds or flows along this interface, depending on the surface gradient. This also occurs at the snow-firn interface, due to the permeability contrast between the seasonal snowpack and the underlying firn.

As the melt season progresses, ablation of the seasonal snowcover exposes glacier ice in the ablation area. The area of ice exposure expands upslope through the summer. Water drains efficiently in the bare-ice zone, typically through sinuous, ice-walled surface channels. These channels can discharge off the front or lateral margins of a glacier, but they more commonly drain into crevasses or moulins.

The seasonal evolution of the supraglacial drainage system has been analyzed in detail on a number of valley glaciers. In general, the efficiency of drainage through this system increases throughout the melt season, as the snow and firn aquifers become saturated and the snowline retreats (e.g., Nienow et al., 1998). The englacial and subglacial systems follow suit. They are largely inefficient early in the melt season (May, June), as moulins and subglacial drainage tunnels have to melt out anew each summer. This gives substantial delays to the drainage of water that drains into the glacier. Once the 'plumbing' is re-established through the flushing of sufficient water through the system, drainage pathways are typically rapid and direct in valley glaciers. Meltwater that drains at high elevations in an icefield may follow a more tortuous, multi-day path to the glacier terminus.

2.2.2 Hydrology of Glacierized Basins

Glaciers delay melting and runoff from seasonal snow until late in the summer. Within a glacierized catchment, they also supplement rainfall and seasonal snowmelt with meltwater from glacial ice. Within a given glacier, there can be year-to-year variations in meltwater storage and runoff. However, a few generalizations are possible (e.g., Fountain and Tangborn, 1985; Hock et al. 2005).

Diurnal Variability

Glacier runoff has a pronounced diurnal cycle on small alpine glaciers, due to the radiation-driven diurnal melt cycle. There is typically a delay of several hours between peak melting and peak runoff, as measured by discharge at the glacier terminus. On larger glacier systems, delays can be much greater and the discharge is more diffuse, due to the distribution of path lengths and hydraulic efficiencies in different parts of the glacier drainage system.

Seasonal Variability

The glacier drainage system evolves on seasonal timescales. Early in the melt season, the drainage system does not yet have the capacity to drain the influx of surface meltwater and there is temporary storage of meltwater on the surface, englacially, and at the bed. As the melt season progresses, saturation of the snow and firn aquifers and elimination of the supraglacial snow cover cause increased inputs to the englacial and subglacial systems,

which develop increased connectivity and a greater drainage capacity. Glacier discharge exceeds meltwater inputs as stored water is evacuated. Late in the melt season, stored water has been flushed and the mature drainage system is highly efficient, leading to rapid throughput and daily discharge totals similar to the daily meltwater inputs.

Through the winter, meltwater shuts down on glaciers in the Rockies. Void of water, subglacial and englacial conduits creep closed and the channelized drainage system in most valley and outlet glaciers shuts down. Free water is still present at the base of the glacier throughout the winter and is sometimes evident through trickling subglacial outlet streams or artesian upwellings in the glacier forefield, signalling drainage through the shallow groundwater system. Most glacial streams freeze up in the winter, with negligible discharge, although some streams remain active underneath a mantle of river ice and snow.

On alpine glaciers, this seasonal evolution of the drainage system is associated with a general increase in the rate of water transport through the glacier system. On the Haig Glacier, for example, the lag between peak melting and discharge was measured at 5 to 7 hours in May and 3 to 4 hours in August (Shea et al., 2005). Overall, the annual hydrograph from a glacial stream shows a large seasonal cycle, with almost all of the discharge concentrated in a few months in the summer season, building to a crescendo in late summer when ablation is highest and glacial storage is minimal. Strong diurnal cycles punctuate this seasonal pattern. Figure 4 illustrates this at Haig Glacier, based on 10-minute stream-gauge data. Shea et al. (2005) describe the field site and methods in detail. The forefield stream typically melts open in late June and shuts down in September, so this plot captures most of the summer runoff from the glacier.
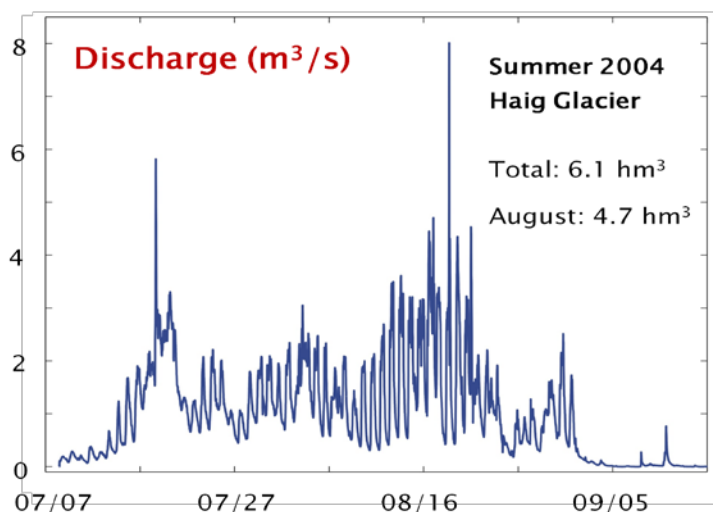
Figure 4. Stream discharge, Haig Glacier, Summer 2004.

This hydrograph is typical of mid-latitude valley glaciers. Diurnal and seasonal runoff patterns differ in glaciers that lack well-developed englacial and subglacial conduits, such as those that drain primarily through the groundwater system. Significant delays in meltwater routing and evacuation can occur year-round in these systems. There are many

observations of glacial meltwater that is routed through the groundwater system and outcrops downvalley, in springs and lakes, but there are few quantitative measurements to assess the water balance or the timescale of drainage in these settings. Most larger (e.g. 1 km^2 or more) glaciers of the Rockies have well-developed drainage streams, but the extent of meltwater drainage to the groundwater system is unknown.

Annual Runoff

Glacier contributions to runoff can be a significant fraction of total annual discharge in catchments with a large glacierized area. Francou et al. (2000) estimate that glacier melt constitutes 30% of stream discharge in the catchment of Glacier Chacaltaya, Bolivia. Hastenrath and Ames report a value of 50% for the Glacier Yanamery, Cordillera Blanca, Peru. On a larger scale, Marks and Seltzer (2003) estimate that ice melt contributes more than 12% of the annual discharge in the 5000-km^2 Rio Santa watershed in the Cordillera Blanca. Glacier inputs dwindle as one goes progressively downstream in most alpine settings, as a result of glaciers making up a smaller percentage of the landscape.

In the eastern slopes of the Canadian Rockies, Hopkinson and Yonge (1998) report that glacier inputs to the Bow River at Banff can exceed 50% in late summer of a dry year, although glacier melt constitutes only 2% of the average annual. Annual discharge statistics therefore mask the importance of glacier contributions to stream flow. In most summers in the Canadian Rockies, seasonal snow persists until July at low elevations on the glaciers, and until August at higher elevations. There is little seasonal snow remaining elsewhere in the mountains at this time. Once this snow cover is removed, glacier runoff is dominated by melt from the low-albedo glacier ice. In summers of drought, groundwater recharge and ice melt are the sole sources of sustenance for the mountain streams.

Glacier runoff is proportional to available melt energy, whereas runoff in non-glacierized catchments is governed by precipitation. This means that discharge from glacierized catchments is less sensitive to weather fluctuations, with a supply of runoff in periods of drought that is lacking in other non-glacierized catchments. Total annual runoff in glacierized catchments varies interannually as a function of glacier mass balance, depending on whether (i) precipitation is stored as ice (positive mass balance), or (ii) long-term ice storage is tapped (negative mass balance). In the latter case, specific runoff (discharge per unit area of the landscape) from glaciers exceeds that from the rest of the catchment. That is, glaciers offer a supplement to the runoff associated with rainfall and seasonal snowmelt. This may also be true in the first case, despite a positive annual glacier mass balance, as glaciers often act as snow-traps and generate greater annual snowmelt than non-glacierized areas in a catchment.

Interannual Variability

The influences described above lead to a dampening of interannual runoff variability in glacierized catchments. Glaciers offer a buffer in periods of extended drought. The influence of glaciers is proportional to the percentage of the catchment that is glacierized. Over a period of many years, a change in glacierized area (advance or retreat of glaciers) will introduce trends in annual runoff, underlying the year-to-year variability associated

with meteorological conditions. These long-term trends are a function of both the specific discharge and the glacierized area, with the latter influence dominating. For instance, many glacierized catchments have experienced a decline in streamflow in recent decades due to the progressive reduction in contributions from glacier melt. Despite ongoing tapping of the ice-storage reservoir, reduced glacierized area is stunting glacier contributions to runoff, globally (Chen and Ohmura, 1990; Braun et al., 2000) and in western Canada (Moore et al., 2008; Demuth et al., 2008; Comeau et al., 2009).

General Comments on Glacier Water Resources

The contribution of glacier runoff to distal streamflow is often exaggerated. Glaciers offer a vivid element of the landscape and their contributions to surface runoff can indeed dominate in heavily-glacierized catchments, but a distinction needs to be made between the runoff from glacial ice and that derived from the seasonal snowpack. For a glacier in equilibrium, there is no annual gain or loss of ice; the main effect of glacial cover is to creates a more diffuse and extended season for meltwater runoff. That said, sustained glacier retreat does mean that long-term water storage is being tapped to augment the runoff derived from rainfall and seasonal snow. This means that current and future runoff is likely to be less than mean historical runoff. Demuth et al. (2008) and Comeau et al. (2009) provide evidence for this in Alberta's glacier-fed rivers.

3.   Inventory of Glaciers in the Canadian Rockies

3.1 Historical Inventories

The first Canadian glacier inventory was carried out between 1969 and 1974. Canada's Department of Energy, Mining and Resources (EMR) used 1:30,000 to 1:60,000 scale aerial photos to identify perennial snow and ice. The outlines of the identified glaciers were transferred to work maps and later digitized and compiled onto a 1:500,000 scale final map. The 1:500,000 maps are the published product and due to the scale, the area of the perennial snow and ice cannot be found with high accuracy. Furthermore, the published maps do not distinguish between only snow and presence of glacial ice. Glacier type (i.e. valley, cirque and hanging) is also not included in the final product. In total the inventory found 1524 areas of perennial snow and ice in the Nelson River catchment (Ommanney 1978). As the project came to a halt in 1974, some areas remained unaccounted for. Glaciers north of the Nelson River Drainage basin were not counted or mapped in this first effort; therefore, glaciers of significant size in the Athabasca and Peace River basins were excluded until later inventory.

In a subsequent effort, Natural Resources Canada (NRCan) produced 1:50,000 scale topographic maps of the Canadian Rockies. Glaciers from these maps were later digitized. This glacier layer is also not without its problems. For instance, it was produced using maps ranging from 1969 to 1998 (Shea et al., 2004), a period during which glaciers experienced extensive retreat. Many of the glacier outlines are therefore not representative of contemporaneous or present extents and temporal resolution can be considered poor. The compilation of Shea et al. (2004) did point out some important

statistics regarding the glacier size distribution: a total count of 3271 glaciers in the Rocky and Columbia Mountains of Alberta and B.C. covered an area of 4298 km^2, giving an average glacier size of 1.3 km^2. This means that the majority of glaciers in the interior ranges of western Canada are small and vulnerable to ongoing retreat.

3.2 Updated Maps of Glacier Coverage

The most recent and thorough inventory of glaciers in western Canada is the recently-completed compilation of Bolch et al. (2010) as part of the Western Canadian Cryosphere Network (WC^{2}N). This dataset has been contributed as a public resource to the Global Land Ice Measurement from Space (GLIMS) glacier inventory (http://www.glims.gov). We refer to this dataset as the WC^{2}N or Bolch et al. (2010) inventory. Two complete time slices have been compiled for the glaciers of Alberta and B.C., 1985 and 2005. The 1985 data is based on glaciers images digitized from aerial photos as a part of a B.C. Provincial mapping program (TRIM). The 2005 compilation is based on Landsat TM5 imagery from 2004-2006. Glacier outlines were updated using an automated process in a GIS. Gross errors due to cloud cover and debris cover were manually corrected. The glacier outlines have also been clipped into different flowsheds with the use of a 100-m DEM.

A similar approach to the one used by WC^{2}N has previously been used in Switzerland. It was done using Landsat 7 ETM+ (Enhanced Thematic Mapper) and Terra satellite's ASTER (Advanced Spaceborne Thermal Emission and Reflection Radiometer) sensor images in conjunction with new techniques for image processing in GIS software to automate the process of making glacier outlines (ETM+) and DEMs (ASTER) (Kaab et al., 2002). This project served as a pilot study for WC^{2}N. A value of 3% error was found for debris-free ice (Paul et al., 2002). Although metadata for the Canadian cordillera WC^{2}N file does not give the error, the similarity in methods would suggest that it is also ~3%.

In comparison to the NRCan glacier layer, WC^{2}N outlines appear to be of higher resolution and have less smoothed borders (Figure 5). It follows that the WC^{2}N inventory and glacier outlines are the best option for both spatial and temporal resolution. Although the WC^{2}N file is the best option for glacier area analysis, it is not without some shortcomings. For example, the Canadian Cordillera WC^{2}N inventory only accounts for glaciers larger than 0.05 km^2. This is consistent with research done by Meier and Bahr (1996), where it was found that even in relatively complete glacier inventories, small glaciers are often overlooked. Hydrologically, these small ice masses behave as glaciers (accumulating and storing snow, then releasing it as snow- and ice-melt), but these ice bodies are not accounted for here. Many are no longer extant, and ice volume estimates based on exclusion of small glaciers should not lead to significant error, as glaciers greater than 1 km^2 represent the majority of the total area. However, it may make a comparison with older inventories more difficult as some data is missing. For example, 741 distinct perennial snow and ice patches exist in the WC^{2}N file for the Nelson River catchment, vs. the 1524 found in the EMR maps.

At present, the WC^{2}N glacier inventory of the Canadian Cordillera is under an embargo period while the PIs investigate recent volume loss in B.C. (Schiefer et al., 2007; Bolch et al.,

2010). As members of WC²N, we have access to this file to carry out the Alberta ice volume estimation.   We base this on the 2005 maps to give a near-present day snapshot.
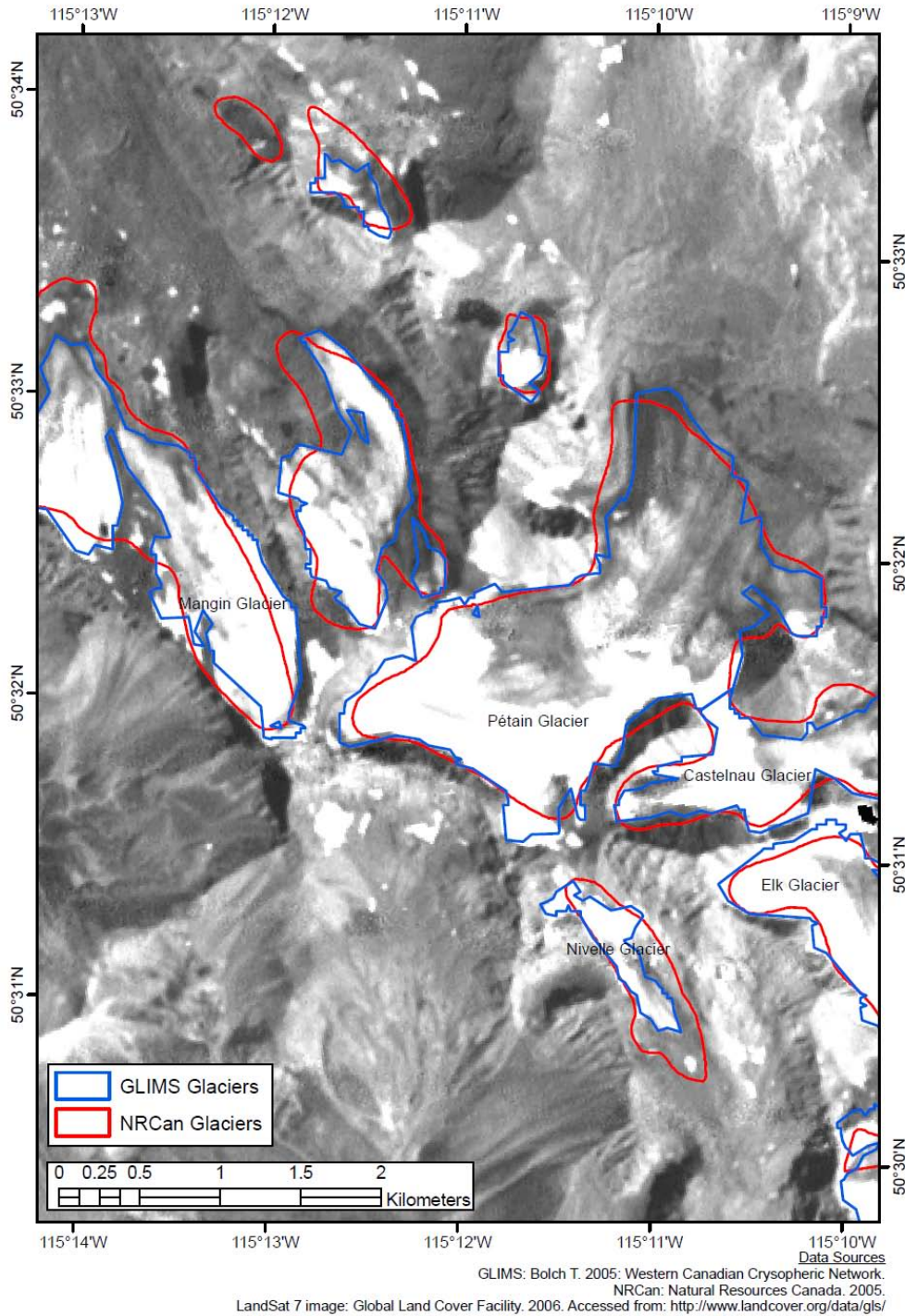
Figure 5. A comparison of the two completed Canadian Cordillera shapefiles (NRCan and WC²N). Note the smoothing in the NRCan layer in comparison to the WC²N map.

3.3 Area and Number of Glaciers in Alberta

3.3.1 Glacierized Area

The 1985 and 2005 WC[2]N glacier inventories offer tremendous insights into the extent of glaciation in B.C. and Alberta and the recent dramatic changes in this glaciation. We discuss the historical changes in glacier cover in a later section. Here we focus on the near present-day (2005) snapshot of glacier extent and glacier-terrain characteristics in Alberta.

Bolch et al. (2010) estimate a total of 17,595 glaciers in B.C. and Alberta in 2005, covering 26,728 km^2. Most of these glaciers reside west of the continental divide; the 2005 inventory identifies 1167 glaciers in Alberta, covering an area of 786 km^2. It should be noted that glacier counts are inherently ambiguous; a contiguous ice mass can be counted as a single entity or it can be subdivided into multiple glaciers based on ice divides and flow directions. Furthermore, as glaciers retreat they are disintegrating at many sites, leading to a reduced glacier area but a higher glacier count as fragments become isolated. Bolch et al. subdivide their ice masses based on ice divides, and they also count isolated glaciers separately. Fragmentation of ice masses gave rise to an increase in Alberta's glaciers from 926 to 1167 over the period 1985 to 2005, despite a 25.4% loss in total glaciated area (see Section 5). We based our analysis on the glacier coverage maps of Bolch et al. (2010), but perform our own subdivision of Alberta's glaciers, identifying 741 independent ice masses covering 791 km^2 in the 2005 inventory (Table 1). This is inconsistent with the glacier count of Bolch et al., but our estimated glacier areas are in good agreement.

Table 1 also compiles statistics on the present-day (~2005) area distribution of Alberta's glaciers. This is telling; of Alberta's 741 remaining glaciers, 81% are smaller than 1 km^2. These small glaciers account for only 23% of the glaciated area in Alberta, while the 14 major icefields and valley glaciers that are larger than 10 km^2 make up 34.7% of the total glaciated area. Table 2 compile the same information but including the B.C. portions of the Peace River basin that drain eastwards into Alberta. Inclusion of these ice masses raises the glacier count and area to 1010 and 960 km^2. Neglecting the arbitrary political border that separates northern AB and B.C., Table 2 offers a more realistic inventory of the glacier water resources that feed Alberta's rivers.

Table 1. Alberta glacier area statistics, 2005, from the WC[2]N inventory.

Size Range (km^2)	Glacier Count		Glacier Area	
	Number	%	(km^2)	%
0.05 − 0.1	109	14.7	8.0	1.0
0.1 − 0.5	378	51.0	90.6	11.4
0.5 − 1.0	116	15.7	83.3	10.5
1 − 10	124	16.7	334.9	42.3
10 − 40	14	1.9	274.6	34.7
Total	741		791.4	

Table 2. Glacier area statistics, 2005, for the entire eastern slopes of the Canadian Rockies, including B.C. portions of the Peace River Basin.

Size Range (km^2)	Glacier Count		Glacier Area	
	Number	%	(km^2)	%
0.05 − 0.1	165	16.3	12.1	1.3
0.1 − 0.5	525	52.0	125.6	13.1
0.5 − 1.0	150	14.9	106.5	11.1
1 − 10	154	15.2	406.1	42.3
10 − 40	16	1.6	309.8	32.3
Total	1010		960.1	

As noted in the methods section, the WC²N inventory does not include glaciers smaller than 0.05 km²; however a question of completeness down to the level of 0.05 km² still remains. Work by Meier and Bahr (1996) suggests that for a complete inventory, the number of glaciers should increase with decreasing area on a log-log chart. If this is true, then the smallest category of glacier should have the greatest number of glaciers. In observing the log-log plot of glacier number vs. area (Figure 6), we see that this is not the case. The WC2N inventory for Alberta levels off at around 0.1 km² and then decreases at smaller areas. This, according to Meier and Bahr (1996), shows that in the range of 0.05-1 km² the inventory is incomplete. This is a point of interest in terms of the results of the inventory but should not significantly affect the estimate of total glacier area and volume estimate, as most of the ice is clearly stored in the larger (> 1km²) glaciers.
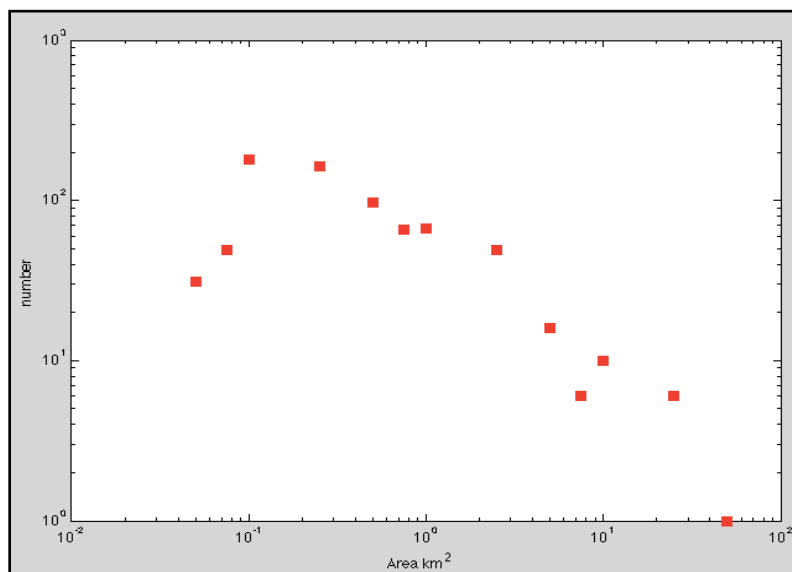
Figure 6. Distribution of the number of glaciers with a given area range versus area. Area bins start at the minimum size characterized by WC^{2}N (0.05 km^2).

For analyses of glacier water resources or sea-level impacts of changing glacier cover, glacier volume is the primary variable of interest, rather than glacier area or glacier count. Unfortunately, this cannot be readily estimated from remote-sensing imagery. To estimate glacier volume in Section 4, we apply local ice thickness-surface slope relationships and area-volume scaling relationships, based on an adaptation of existing theory to the specific case of the Canadian Rockies. These methods require characterization of the glaciated terrain (e.g., elevation distributions, surface slopes, and glacier types), for which we use a 100-m digital elevation model (DEM) of the region. The next section describes the terrain characteristics of the 2005 glacier cover in the eastern slopes of the Canadian Rockies. Unless stated otherwise, we include B.C. portions of the Peace River Basin in most of the analysis that follows.

3.3.2 Terrain Characteristics of Glaciers in the Eastern Slopes of the Rockies

Glacier cover on the eastern slopes of the Rockies spans elevations of 1556 to 3721 m, the latter being the Alberta's high point, Mt. Columbia. The median elevation of the province's glaciers is 2620 m; 50% of Alberta's glaciated area lies above this elevation and 50% below. The minimum and median elevations of Alberta's glaciers decrease with latitude, reflecting the cooler temperatures and shorter, less intense summer melt season in northern Alberta. Glaciers extends to lower elevations at the higher latitudes of the B.C. portions of the Peace Basin, with the median glacier elevation in the Peace Basin, 2208 m, considerably lower than that of Alberta's glaciers.

In Table 3 we separate the glacier cover in each of Alberta's glaciated basins: the Bow, Red Deer, North Saskatchewan, Athabasca and Peace. Alberta's glaciers are concentrated in the headwaters regions of the North Saskatchewan and Athabasca Rivers, with over 77% of the glacierized area found here. Much of this is in the Columbia Icefields region. Headwaters regions of the Peace River in northern B.C. also contain significant amounts of glacier ice.

Table 3. Glacier area and elevation distributions for Alberta river basins, based on the WC^{2}N glacier inventory for 2005.

| Basin	Count	Area (km^2)	Elevations (m) min	median	max
Bow	96	60.3	1972	2620	3473
Red Deer	22	16.6	2441	2729	3084
North Saskatchewan	258	286.2	1566	2610	3464
Athabasca	271	321.3	1556	2560	3721
Peace (AB)	94	107.6	1640	2457	3270
Peace(AB and BC)	363	276.6	1424	2208	3270
Alberta	741	792.0	1550	2620	3721
All eastern slopes	1010	961.0	1424	2507	3721

Figure 7 plots the hypsometry (area vs. elevation distribution) of glacier cover in each basin and for the whole region. Basin-scale glacier hypsometry provides baseline data that are required for regional estimates of glacier mass balance and climate sensitivity (Section 5). These data reveal that most of the glacier ice on the eastern slopes resides at an elevation range of 2300-2800 m asl. The end-of-summer snowline, or equilibrium line altitude (ELA), is typically found at these elevations in the Canadian Rockies, although the ELA frequently rises above these elevations.
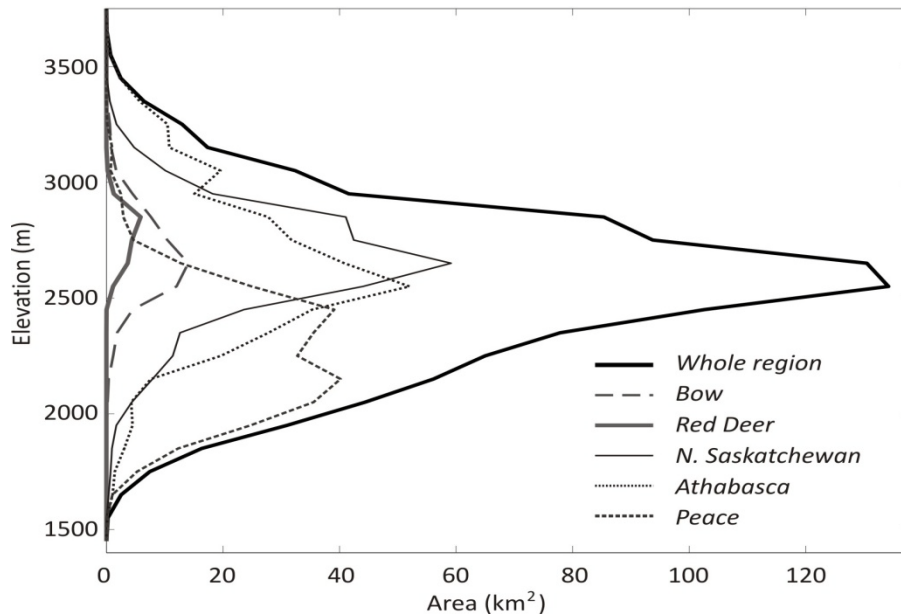
Figure 7. Glaciated area vs. elevation for 100-m elevation bins in Alberta's glacierized river basins.

Glacier aspect is another factor that is critical to glacier melt, as north-facing slopes experience less incident solar radiation and a less energetic melt regime. The distribution of Alberta glaciers by aspect is given in Figure 8. Because we are analyzing only the eastern slopes of the Rockies, there is a strong easterly component to the ice cover. Despite this bias, Alberta's glaciers are predominantly north facing, with 60% of the glaciated area having a northwesterly, northerly, or northeasterly aspect.

This aspect distribution does not come into play in the current analysis, but glacier aspect is important to physically-based (energy balance) melt modelling for glacier mass balance simulations. In Section 5 we present empirically-based mass balance scenarios for historical and future glacier change in Alberta. This provides first-order estimates of the water resources impacts of ongoing glacier retreat, but we recommend follow-up work that includes physically-based simulations of glacier response to climate change.
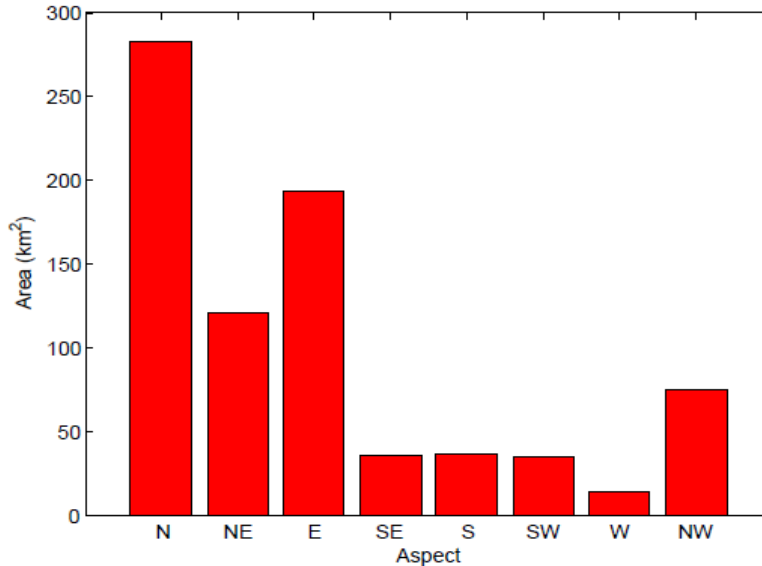
Figure 8. Glaciated area as a function of aspect in Alberta.

3.4 Classification of Glacier Type

The most common method for estimating glacier volume from glacier area is to use empirical scaling relationships based on available ice-thickness (volume) data. Bahr et al. (1997) have also conducted theoretical analyses to support these empirical models, but the volume-area relationship is intrinsically related to the type of glacier. We therefore made an effort to classify the glacier inventories by type: cirque glaciers, hanging glaciers, valley glaciers, or icefields.

We explored this based on historical EMR maps of the Nelson River basin, making the assumption that the distribution of ice masses in this basin is representative of Alberta's glaciers. Using Google Earth™, we compared perennial snow and ice from the EMR maps to modern (2002 onward) satellite imagery. To create a catalog, the location of perennial snow and ice on the EMR maps is found on the satellite images. The location is recorded and then classified into glacier or snow if easily visible. If the feature is classified as a glacier, it is then further classified into type of glacier (cirque, valley, hanging, or icefield). This classification scheme is a simplified version of the GLIMS glacier classification scheme given in Rau et al (2005). In locations with high-resolution, late summer/early fall satellite images, classifications were straightforward and were based on the presences of visible ice features such as crevasses and bergschrunds. In other locations, winter scenes or low-resolution images make it difficult to clearly discriminate between snow and ice, and to distinguish the glacier type.

All identified perennial snow and ice bodies from EMR map sheets 4*5A, 4*5B and 4*5C were classified for this analysis. This area includes the Old Man River, Red Deer River and Bow River catchments. Due to difficulties with low resolution satellite images, not every

location on the EMR maps can be definitively classified into "snow", "glacier", or "deglaciated". In total there are 662 snow and ice features on the three EMR maps. Of the 662 points, 403 reside within regions with high-resolution satellite imagery, but only 151 glaciers could be clearly identified and categorized (Table 4). Within the areas with high-resolution imagery, 41 (~10%) of the original snow/ice patches are no longer present.

These results underscore the numerical significance of different types of glaciers. Each of these glacier types is expected to contribute significantly to the total glacier area in the Rockies. This is consistent with other regions. For example, cirque, valley, and hanging glaciers make up 42%, 30%, and 17% of the total glacier area in the Nan-Shan Mountains of southern China (Lewandowski and Zgorzelski, 2004).

Table 4. Glacier class numbers and percent of 192 definitive glaciers in the Old Man, Bow, and Red Deer River basins from the EMR maps.

Glacier Type	Number	Percent
Valley glaciers	56	37.1
Cirque glaciers	49	32.5
Hanging glaciers	36	23.8
Icefields	10	6.6
Deglaciated	41	

The volume-area scaling method used to approximate glacier volume (Section 4) was developed for valley glaciers and icefields. It is not known whether these relationships work well for cirque and hanging glaciers; however, for the scope of this project, a first assessment of volume will be made through the valley-glacier and icefield scaling relationships, treating cirque and hanging glaciers as valley glaciers. There is little basis to choose otherwise at this time, but future work should address the suitability of the valley glacier relationship to different glacier morphologies.

4. Glacier Volume in Alberta

As discussed in Section 2, glacier volume measurements require a labour and capital-intensive approach. Volume-area (*V-A*) and other scaling relations have been derived from the available global ice-thickness data. The following section describes the theory behind the scaling relations and the use of these methods to calculate ice volume.

4.1 Methods of Estimating Glacier Volume

4.1.1 Volume-Area Scaling Theory

Based on empirical volume data from 63 glaciers around the world (seismic and radar), Chen and Ohmura (1990) derived the following curvilinear relationship between glacier area and volume:

$$V = cA^b,\qquad\qquad(1)$$

where V (10^6 m^3) is the volume and A (km^2) is the surface area of the glacier. In their analysis they found c to be 28.5 and b to be 1.357. As the data used to derive these constants is from many different regions, the values for c and b can be considered a sort of world average and c, in particular, needs to be adjusted regionally (Clarke et al., 2009). To give an idea of the regional variability in c, Chen and Ohmura found a value of 16.1 in the Alps and 48.0 in Svalbard.

This relationship is rooted in the relatively well-understood, rheologically-determined surface profile and aspect ratio of valley glaciers, and it is believed to be generally applicable to a large ensemble of glaciers. However, individual glaciers can deviate dramatically from this relationship as a result of complex or deeply eroded bed topography, unusual ice flow regimes (e.g., extensive glacier sliding), or as a result of being far out of equilibrium. The relationship is not intended to be used on individual glaciers and Meier et al. (2007) estimate an error of 50% for a single glacier volume. When applied regionally or globally, Meier et al. (2007) suggest that the error is reduced to approximately 25%.

Radic et al. (2008) carry out a systematic analysis of the effects of glacier disequilibrium in volume estimates from *V-A* scaling. This study supports the conclusions of Meier et al. (2007), with errors of up to 57% in modelled volume for individual glaciers, but reasonable results were obtained for an ensemble of glaciers. The use of regional *V-A* scaling is only valid if effects such as climatic disequilibrium, bedrock topography, and ice dynamical regime have no systematic bias. We consider these assumptions in the following section.

4.1.2 Inversion of Ice Thickness from Surface Slope

As an alternative to *V-A* scaling, first-order approximations of ice thickness can be made from the surface slope, based on the empirical observation that glaciers typically have a gravitational driving (shear) stress, τ_d, of about 10^5 Pa at the base (Paterson, 1994). This uniform driving stress is due to the rheology of glacial ice; ice deforms through non-linear

viscous flow, with an effective viscosity that allows glacial ice to support a shear stress of approximately 10^5 Pa. Glaciers thicken until they reach stresses of this magnitude, and further thickening or steepening of the ice surface leads to increased ice flow and thinning. Taking advantage of this relation, it is possible to estimate local ice thickness, H, through the equation

$$H = \frac{\tau_d}{\rho g \nabla s},$$ (2)

where ρ is the ice density (910 kg/m^3), g is gravity, and ∇s is the surface slope.

In reality, local basal stresses deviate substantially from 10^5 Pa, due to stress bridging, the influence of longitudinal and horizontal stresses, valley shape, and the effects of basal sliding or subglacial sediment deformation. Small ice patches and the low-sloping accumulation areas of icefields commonly exhibit lower shear stresses ($\tau_d < 10^5$ Pa), while larger glaciers and steep valley glaciers can have shear stresses well in excess of 10^5 Pa. Given enough data to test and calibrate such relations, it could be possible to include some of these effects in estimates of ice thickness for individual glaciers. In the absence of such data however, we adopt a similar approach to the *V-A* scaling, applying Eq. (2) to the population of glaciers with the assumption that 10^5 Pa is representative for a large sample of glaciers within a mountain region.

To use this ice thickness-surface slope relation, we calculate surface slope from DEMs, permitting an estimate of ice thickness for each glacierized cell in the DEM. It is not clear whether local or glacier-averaged slopes are more appropriate for this calculation. The relation is local by definition, but it breaks down when surface slopes approach zero (infinite ice thickness), as occurs in the accumulation area of large icefields and ice sheets. Estimates based on glacier-averaged slopes are not glaciologically realistic – they give a uniform ice thickness across an entire glacier – but they may be representative of the average glacier thickness. We therefore apply this method using both local and glacier-averaged surface slope, providing two different estimates of ice thickness. Ice volume is then calculated from the mean glacier thickness times the glacier area.

4.2 Application to the Canadian Rockies

Application of the local slope-thickness relationship in Eq. (2) is straightforward. Individual glacier volumes are estimated for the local and mean slopes. We then aggregate the volume estimates by river basin (Table 4).

Volume-area scaling in Eq. (1) is also applied to individual glaciers, but the choices for scaling parameters c and γ are uncertain. Based on previous research, the global *V-A* scaling relation can be applied to the Canadian Rockies with an estimated aggregate (regional) uncertainty of 25%. We use these as the basis for one estimate of glacier volume, following Demuth et al. (2008) and Comeau et al. (2009). To provide an estimate of the sensitivity to the scaling parameters, we also consider regional values of c and γ applied by Hopkinson

and Young (1998). These are based on a subset of 32 mountain glaciers in the global inventory, primarily from sites in North America.

The global and regional values of c and γ are not necessarily applicable to the carbonate geology and style of glaciation in the Canadian Rockies, which are characterized by low-sloping icefield accumulation areas drained by deeply-incising valley/outlet glaciers. Most of the glaciers used by Hopkinson and Young (1998) are situated in the Cascade Mountains of the Coast Range, and only three glaciers are situated in the Rocky Mountains. It is not clear that the volcanically-generated topography, geology and maritime climate of the Coast Range should give scaling coefficients that are representative of the Rockies. However, we do not have sufficient ice-volume data from the Rockies to develop locally-applicable relations.

Application of the local and average glacier slopes (Eq. 2) gives glacier volume estimates of $67\,\mathrm{km^3}$ and $43\ \mathrm{km^3}$ for the entire region, whereas the world aggregate and North American *V-A* scaling relations give volume estimates of 49 and $59\ \mathrm{km^3}$, respectively (Table 4). Irrespective of method, the 10 largest glaciers contain more than 48% of the total glacier volume. We have no reason to favour any one of these four estimates, so we average these values and arrive at an estimate of $55 \pm 15\ \mathrm{km^3}$, with this error term based on the recommendation of 25% under *V-A* scaling theory, including the compounding effects of the estimated 3% error in the ice-area reconstructions. This error estimate also brackets the four individual estimates of glacier volume in the eastern slopes.

Our best estimate of glacier volume, $55\ \mathrm{km^3}$, corresponds to an average glacier thickness of $57\,\mathrm{m}$. Of this ice volume, $47 \pm 13\ \mathrm{km^3}$ is within Alberta (Table 5) and the remaining $8\ \mathrm{km^3}$ is in B.C. portions of the Peace River headwaters region.

Table 4. Glacier volume estimates for Alberta's river basins from different slope-thickness and volume-area scaling relationships. This includes glacierized portions of the Peace River basin in B.C.

Method	c	b	Volume ($\mathrm{km^3}$)
Global aggregate scaling parameters	0.0285	1.357	49
North American scaling parameters	0.0308	1.405	59
Local slope-thickness estimate			67
Glacier-averaged slope-thickness estimate			43

4.3 A Rockies-Specific Scaling Relation?

Glacier thickness data is available from six sites in the Rocky Mountains: the Grinnell (Montana), Dinwoody (Wyoming), Haig, Rae, Peyto, and Athabasca Glaciers. The latter four are in Alberta. The Athabasca Glacier is an interesting case because it is anomalously thick (ca. 300 m in places). For this reason it is an outlier on the world aggregate power law formula derived by Chen and Ohmura (1990), and it is excluded from the global composite of glaciers that inform this relation.

We suspect that the Athabasca's unusual depth is due in part to its size (roughly 8 km^2) and the fact that it transports large fluxes of ice from the Columbia Icefield (Figure 9). However, the anomalous ice thickness may also be due to the low competence of the underlying carbonate rocks, leading to a deeply eroded (overdeepened) bed. Radar data from Haig Glacier indicates similarly anomalous depths, with a maximum ice thickness of just over 200 m. While this is only two sites, these results indicate that c and b may need to be adjusted for application of volume-area scaling relations to the Canadian Rockies.


Figure 9. The Athabasca Glacier, Canadian Rockies, August 2009.

For this report we spent considerable effort exploring the possibility of developing local, Rockies-specific volume-area scaling parameters. Figure 10 shows the $V\text{-}A$ relationship for five of the Rockies glaciers. Peyto Glacier data has been excluded because it is contentious; Holdsworth et al. (2006) report an estimated average ice thickness of 95 m along the glacier centreline, a value adopted by the world glacier inventory (Ommanney, 2002), but the data is primarily from the ablation area rather than the complete glacier system. Furthermore, the *average* (vs. centreline) glacier thickness in the portion of the glacier sampled by Holdsworth et al. (2006) is about 50 m, which is unexpectedly low.

The power-law fit to this data gives c = 0.0506 and b = 1.666. In keeping with the Athabasca Glacier anomaly, this new scaling relationship gives a higher coefficients than the world aggregate values (c =0.0641 and b =1.369). The coefficient of determination (R^2) for the new relationship is 0.97, meaning that 97% of the variation in the volume is explained by the $V\text{-}A$ scaling relationship. The power law fit is stronger than a linear fit

through the data, but we are deeply limited by the paucity of ice-thickness observations in the Rockies and this relationship is heavily swayed by the Athabasca data point. Including Peyto Glacier data in the regression swings the relationship the other way, with an exponent of b = 1.002: essentially a linear relationship, which is known to be inappropriate to glacier V-A scaling (e.g., Bahr et al., 1997). This sensitivity to the addition or removal of a single glacier undermines confidence in the local V-A scaling relation of Figure 10. We conclude that we do not have adequate ice-thickness data to follow this approach further at this time, but recommend that such measurements be pursued in order to increase confidence and reduce the error bars in ice volume estimates for the Rockies.
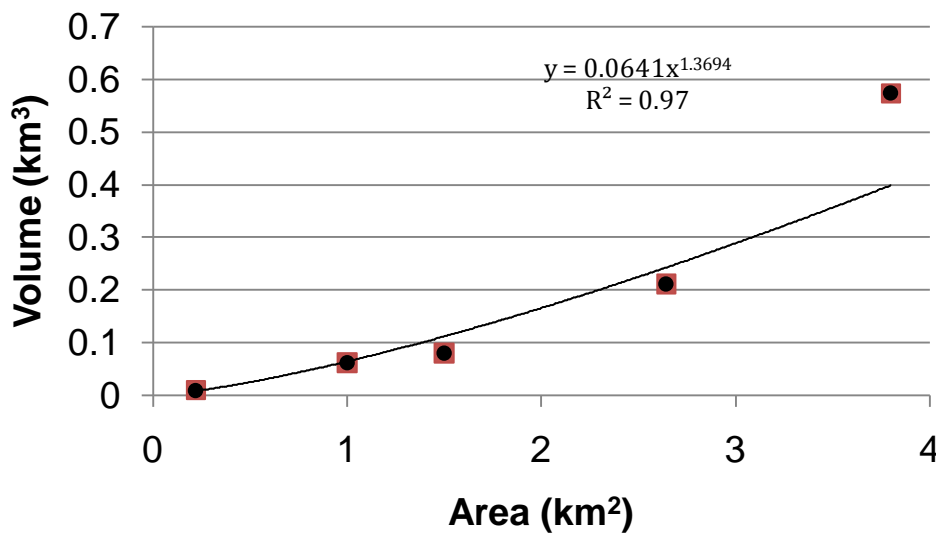
Figure 10. Volume-area relationship for Rockies glaciers. Plotted from left to right are the Rae, Grinnell, Dinwoody, Haig and Athabasca Glaciers. The Rockies-specific scaling relationship has the parameters *c = 0.0641* and *b = 1.3694.*

4.4 Ice Volume Estimates by Hydrological Basin

Table 5 presents ice volume estimates for each glacierized hydrological basin. Note that the GIS discretization gives a slightly different total area estimate when clipped by catchment, compared to the region-wide assessment in Table 1. We present the full range of ice volume estimates for each basin as there is no good objective basis to favour any one of the ice-volume reconstructions in Table 4.

Table 5. Glacier area and volume estimates for Alberta river basins, based on the WC^{2}N glacier inventory for 2005. Best estimates are based on the mean prediction from the four volume estimation methods, and modelled values are explained in Section 6.

| Basin	Area (km^2)	Glacier Volume (km^3)		
		Range	Estimate	Model
Bow	60.1	2.1-3.6	3.0 ± 0.7	2.9
Red Deer	16.6	0.6-1.0	0.9 ± 0.2	0.8
North Saskatchewan	286.3	13-19	17.5 ± 4.4	15.6
Athabasca	320.5	12-18	16.7 ± 4.2	19.9
Peace(AB)	107.6	6-14	8.8 ± 1.4	
Peace(AB and BC)	276.7	13-23	16.9 ± 4.2	15.8
Alberta	791.1	35-55	47 ± 13	
Eastern slopes	960.3	43-67	55 ± 15	55.0

5. Recent Glacier Retreat

Here we analyze glacier changes during the historical period (the last four decades) and projected future changes in the glacierized area, glacier mass balance, and meltwater runoff from glaciers in the Rockies.

5.1 Changes in Glacierized Area

Schieffer et al. (2007) and Bolch et al. (2010) examine recent (late 20th century) changes in glacier volume and area in western Canada. The compilation of Bolch et al. documents changes in glacier area for the entire western Cordillera over the period 1985 to 2005, providing a regional context for the changes that we are seeing in the Rockies. Figures 11 and 12 illustrate the B.C.- and Alberta-wide changes in glacier area for this 20-year period, subdivided into major glacier-climate zones.   The southern, central, and northern Rockies in these plots include both eastern and western slopes. These regions experienced a loss in ice cover of about 15% from 1985 to 2005. When Alberta glaciers are isolated, one sees a 25% decrease in glacier area over this period, from 1053 km^2 to 786 km^2.

All regions in B.C. and Alberta are experiencing glacier loss. The greatest total losses occurred in the most heavily glaciated regions, as one would expect. The eastern slopes of the Rockies experienced disproportionately heavy losses: 25% of the total glaciated area vs. 11% for B.C. The reason for this contrast is not well-understood, but probably arises from two main factors: (i) the predominance of relatively small glaciers in Alberta, and (ii) more significant reductions in snowfall in the eastern slope of the Rockies over this period, relative to coastal and interior B.C.
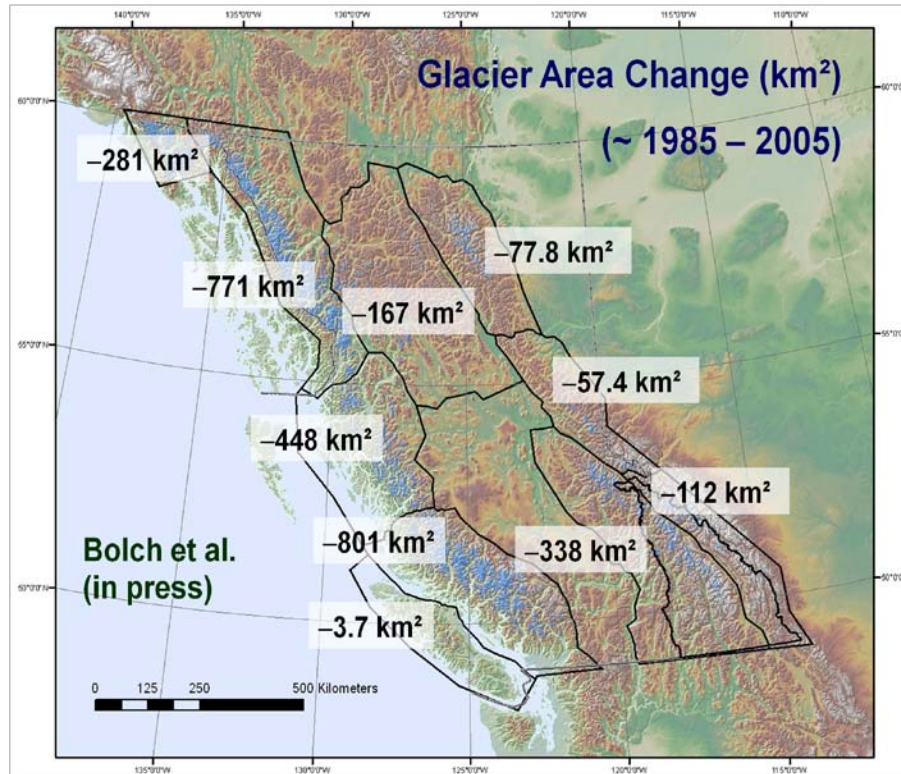
Figure 11. Changes in glacier area in major glacioclimatic regions of B.C. and Alberta from 1985 to 2005.

The average glacier size in Alberta (2005) is 1.14 km². By contrast, the average glacier size in B.C. (2005) is approximately 2.11 km². Small glaciers are known to be more sensitive to climate warming, due to a variety of the positive feedbacks associated with sustained negative mass balance (e.g., loss of the firn layer, darkening of the glacier surface, increased sensible heat flux to the glacier from the surrounding, freshly-deglaciated rock).

Demuth et al. (2008) carry out a similar analysis of Landsat imagery within the North and South Saskatchewan River Basins, using late summer images from 1975 and 1998. This provides a 1975 benchmark, from which we can evaluate recent changes in glaciated area in these critical basins for Alberta and the Canadian prairies. Table 6 summarizes these findings, combining the results of Demuth et al. (2008) and Bolch et al. (2010).

Table 6. Glacier area in the South and North Saskatchewan Basins (km²).

Basin	1975	1985	1998	2005
South Saskatchewan	141	93	89	77
North Saskatchewan	395	324	306	286
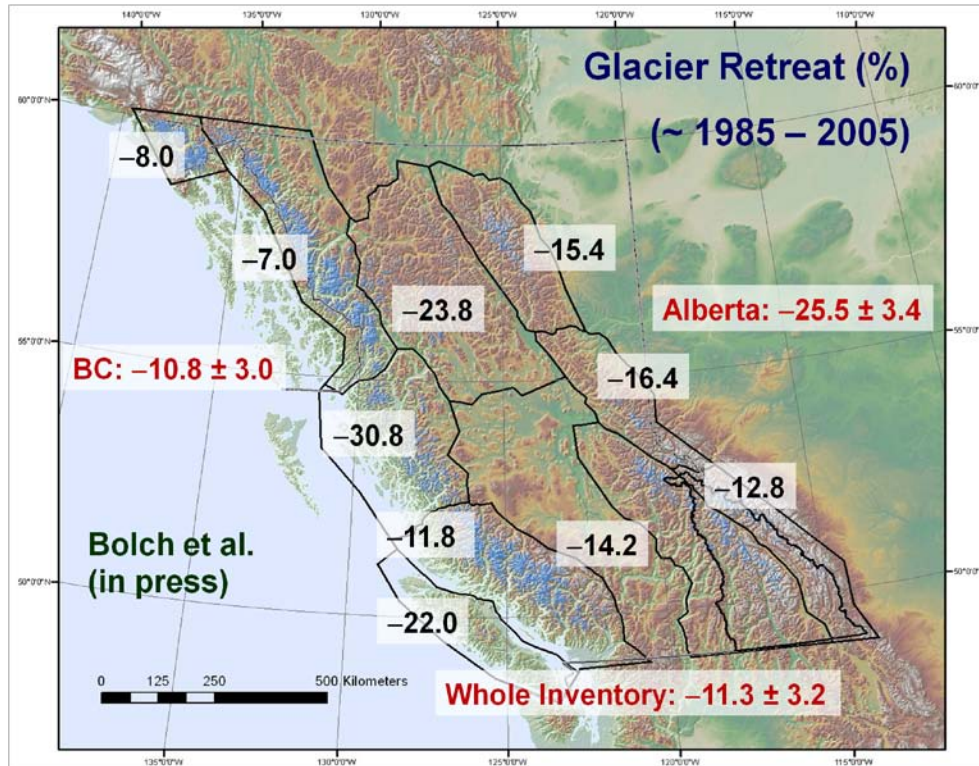
Figure 12. Changes in percentage glaciated area in B.C. and Alberta from 1985 to 2005.

Because glaciated area is an important aspect of glacier contributions to streamflow, this rapid loss of glacier ice is evident in reduced late-summer streamflows in Alberta's rivers (Demuth et al., 2008; Comeau et al., 2009). Glaciers are losing mass, supplementing streamflow, but they are playing a diminishing role in water resources in Alberta. We analyze this in more depth in the following sections.

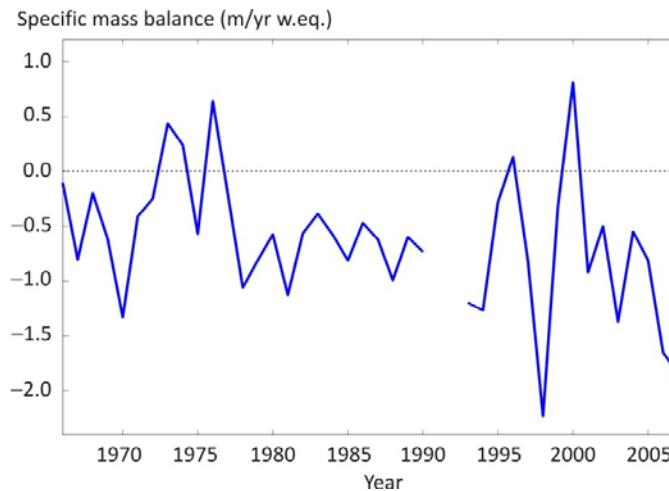## 5.2 Peyto Glacier Historical Mass Balance Data

Glacier mass balance data has been gathered from approximately 310 glaciers worldwide over the past several decades, although only a subset of sites has longterm data. This data is archived through the world glacier monitoring service (http://www.geo.unizh.ch/wgms/). The observations document worldwide glacier retreat in recent decades, similar to what is observed in the Rockies.

5.2.1 Mass Balance Trends from Peyto Glacier

Glacier mass balance has been measured since 1966 at the Peyto Glacier, an outlet of the Wapta Icefield in Banff National Park. Various federal government agencies have contributed to this effort, which currently resides in the experienced hands of Mike Demuth of the National Glaciology Program, Geological Survey of Canada, Ottawa. Demuth

and Keller (2006) describe the Peyto Glacier record in detail. Annual specific (glacier-averaged) surface mass balance data for the period 1966-2007 is plotted in Figure 13. The mass loss over this period has been dramatic: only 5 years had a positive mass balance (a net gain of snow/ice), and the average rate of thinning was −0.63 m w.eq. yr^{-1}. This translates to a cumulative thinning of 29.2 m over the 42-year period, averaged over the whole glacier. The lowest elevations have thinned much more than this. In terms of glacier volume, the estimated loss is 0.365 km^3, or 0.332 km^3 water equivalent.

A linear fit of the data indicates a significant trend of −17.5 mm/yr w.eq per year. This corresponds to more than a doubling of the rate of ice loss over the period 1966 to 2007.

Figure 13. Annual surface mass balance of the Peyto Glacier, 1966-2007.

Seasonal mass balance data that is available from 1966-1995 provides insight into the controls and variability of the mass balance record (Demuth and Keller, 2006). The average annual values for winter, summer, and net mass balance over this period were b_w = 1.20, b_s = −1.75, and b_n = −0.56 m w.eq. yr^{-1}. Interannual variability in net mass balance correlates with both winter and summer values, with linear correlation coefficients of 0.63 and 0.79, respectively. This means that summer mass balance has a larger control on year-to-year variability, but both the intensity of summer melt season and the extent of the winter snowpack are influential in the region (Bitz and Battisti, 1990; Demuth and Keller, 2006; Shea and Marshall, 2007). We discuss correlations with regional (Lake Louise) weather data in section 5.3.

5.2.2 Mass Balance Gradients on Peyto Glacier

Altitudinal mass balance data are also available over the period 1966-1995, providing insight into several key parameters for understanding glacier mass balance: the elevation of the end-of-summer snowline (the ELA), the areal percentage of the glacier that is snow-covered at the end of the melt season (the AAR), and vertical gradients in mass balance. Seasonal and net annual mass balance data are available in 100-m elevation bins for the

Peyto, from 2150 to 3150 m altitude. Based on linear regressions through this data (e.g., Figure 15a) for each year, the average gradients in the winter, summer, and net mass balance from 1966-2005 were:

$$\frac{\partial b_w}{\partial z} = 1.56 \pm 0.49 \text{ mm w.e. m}^{-1},$$

$$\frac{\partial b_s}{\partial z} = 4.56 \pm 0.87 \text{ mm w.e. m}^{-1},$$

$$\frac{\partial b_n}{\partial z} = 6.14 \pm 0.82 \text{ mm w.e. m}^{-1}.$$

Linear fits to the winter and net mass balance data are reasonable and higher-order (e.g. quadratic) fits cannot be justified. We expected that the linear balance gradients would differ in years with positive mass balance vs. years with extremely negative mass balance, but there is no clear pattern here: $\partial b_n/\partial z$ is uncorrelated with b_n ($r = 0.07$). Figure 14b illustrates this for discrete mass balance 'bins', with the mean regression parameters for each bin given in Table 7.
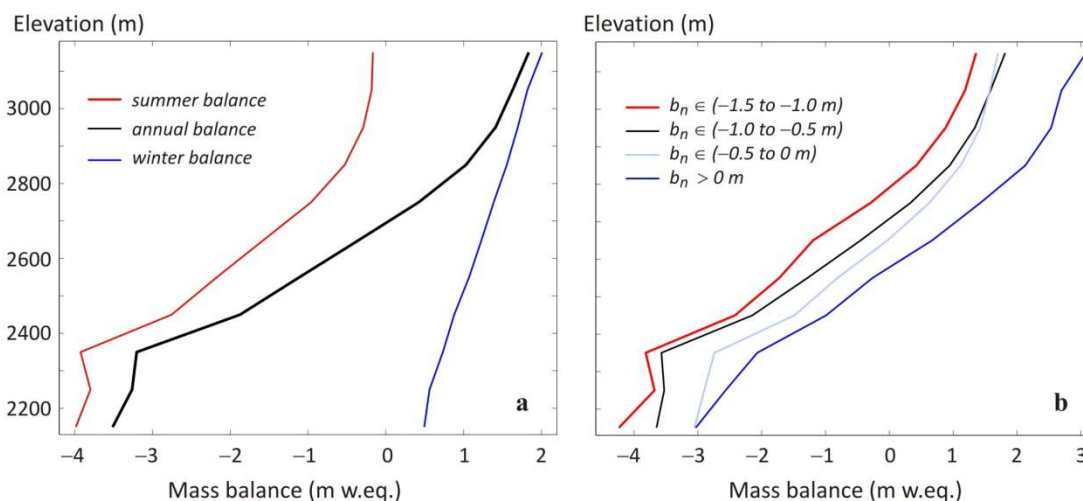
Figure 14. Vertical gradients in net annual mass balance at Peyto Glacier, 1966-1995.

There are no other glaciers in the Rockies with longterm mass balance records, but observations over shorter periods on the Haig and Ram Glaciers are consistent with this data and the overall trend of increasingly negative mass balance. It has become commonplace for smaller glaciers in the Rockies to be bereft of snow at the end of the summer melt season. See for example the frontispiece from the Haig Glacier in September 2009, showing complete loss of the winter snowpack right up to the continental divide. This indicates that these glaciers are completely out of equilibrium with the current climate and have become unviable; glacier thinning and retreat can be expected to continue.

Table 7. Mass balance gradients and meteorological conditions as a function of net annual mass balance for Peyto Glacier.

Net mass balance (m w.eq.)	$\overline{b}_n$ (m)	$\partial\, b_n/\partial\, z$ (mm/m)	$\overline{T}_{JJA}$ (°C)	$\overline{P}_w$ (mm)
< -1.5	−1.91	n/a	12.9	435
−1.5 to −1.0	−1.23	6.24	11.4	374
−1.0 to −0.5	−0.71	6.39	11.2	409
−0.5 to 0	−0.29	5.53	10.9	412
> 0	0.45	6.67	10.8	474

5.3 Mass Balance Relationships with Local Climatology

Longterm meteorological data is available from a small number of Environment Canada weather stations in the Alberta foothills. The most proximal sites to the glaciated regions of the Rockies which have longterm data are Lake Louise (1915-present), Banff (1887-present), and Jasper (1916-present). Within these, Lake Louise is the highest-elevation site (1524 m) and is only 37 km from the Peyto Glacier.

Over the period 1966-2007, the duration of the Peyto Glacier mass balance record, mean annual precipitation in Lake Louise, P, was 573 mm, mean winter (Sept-May) precipitation, P_w, was 414 mm, and mean summer (June to August) temperature, T_{JJA}, was 11.2°C. Here we define winter based on the glaciological mass balance year, September through May. These parameters are known to be important to glacier mass balance, with summer temperatures being the most critical.

For the 42-year record of net annual mass balance at Peyto, linear correlations with the Lake Louise precipitation and temperature give $r\,(b_n, P) = 0.19$, $r\,(b_n, P_w) = 0.20$, and $r\,(b_n, T_{JJA}) = -0.57$. Only the summer temperature is significant, probably because summer mass balance fluctuations are more important in controls of interannual mass balance variability.   Over the period 1966-1995 for which seasonal mass balance data from the Peyto Glacier is available, weather records from Lake Louise indicate the expected influence of winter precipitation: $r\,(b_w, P_w) = 0.58$. As a mass balance diagnostic, winter precipitation totals in Lake Louise are stronger than annual precipitation. For the 42 years of data, $\partial b_n/\partial T_{JJA} = -405$ mm °C^{-1} and $\partial b_n/\partial P_w = 1.43$ mm mm^{-1}.

Table 7 lists the mean summer temperatures and winter precipitation totals for the different historical mass balance categories at the Peyto Glacier described in section 5.2. Years with extreme negative mass balance ($b_n < -1.5$ m) coincide with warm summers, with a temperature anomaly of +1.7°C, while years with positive mass balance are associated with cool summers ($\Delta T = -0.4$°C) and above-normal winter precipitation (+14%). The relationship between b_n and summer temperatures is consistent across categories in Table 6, while winter precipitation has less influence. For example, the years of extreme negative mass balance coincide with a positive anomaly in winter precipitation in Lake Louise (+5%).

Both summer temperature and precipitation have significant trends in Lake Louise over the period 1966-2007: $dT_{JJA}/dt = 0.008°C$ yr^{-1} and $dP_w/dt = -1.4$ mm yr^{-1}. Extrapolated over a century, this corresponds to a warming of 0.8°C and a decrease in precipitation of 140 mm (34%). The trends of decreased winter precipitation and warmer summers both contribute to the declining mass balance at glaciers in the Rockies, and are characteristic of the region.

5.4 Mass Balance Relationships with Synoptic Climatology

In addition to local meteorological conditions, Bitz and Battisti (1999), Stahl and Moore (2006), and Shea and Marshall (2007) demonstrate the sensitivity of glacier mass balance in the Rockies to synoptic patterns of atmospheric circulation. The persistence of specific weather systems has a strong effect on both snow accumulation and summer melt. There are numerous ways to quantify this, but we use 'flow indices': measures of the strength, direction, and vorticity of upper air flow. In addition, the 500-mb height is a measure of the integrated temperature in the air column between the ground and the 500-mb surface, and daily to seasonal variability in the 500-mb height, Z_{500}, is broadly governed by the persistence of either warm, subtropical or cold, polar air masses that impact the Rockies. Warm, dry periods in the summer (e.g., drought conditions of 1998 or 2003) are associated with persistent high-pressure ridging: subtropical air masses in southwestern Canada and high values of Z_{500}.
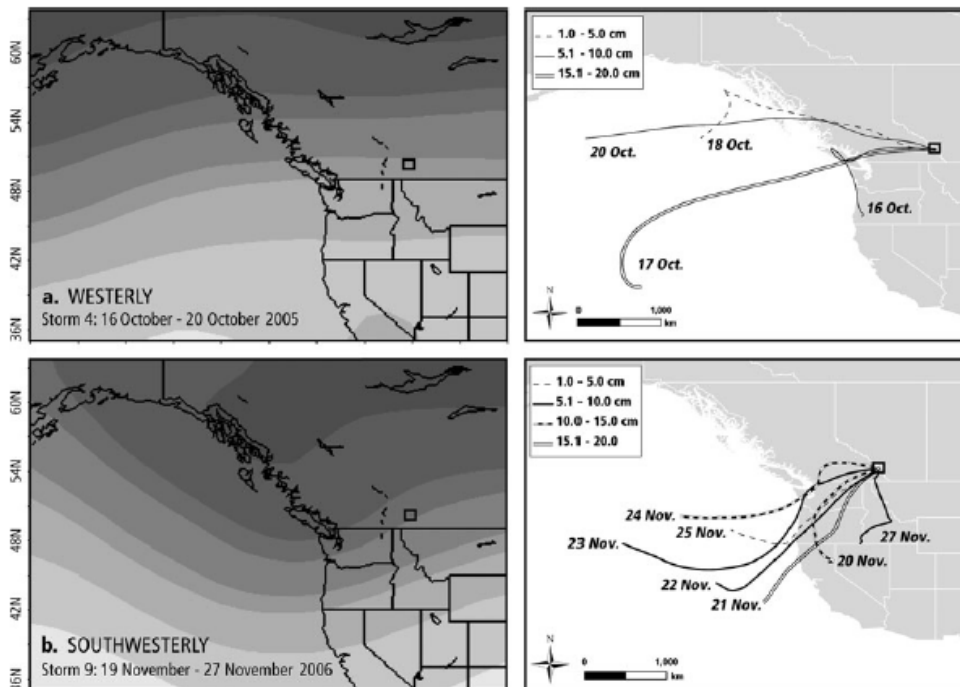
Figure 15. Examples of synoptic meteorological conditions/upper air flow associated with snow accumulation in the Canadian Rockies. Contours on the left indicate 500-mb heights, while panels on the right show air mass back trajectories for two major snow events on the Haig Glacier.

The 500-mb height is also indicative of storm tracks that deliver moisture to the region. When the jet stream is strongly zonal over southwestern Canada, 500-mb heights are low and snow-bearing systems are more frequent. Sinclair and Marshall (2009) discuss this, based on isotopic signatures in the snowpack on the Haig and Opabin Glaciers. Figure 15 gives an example.

Shea and Marshall (2007) demonstrate that synoptic flow patterns can explain much of the mass balance variability on Peyto Glacier. We extend this analysis and develop multivariate statistical relations for net annual mass balance, based on two approaches: (i) a combination of local (Lake Louise) meteorological variables and synoptic flow indices and (ii) purely synoptic flow indices. Linear correlation analyses between time series of Peyto Glacier net annual mass balance and a large selection of meteorological variables reveals the most relevant variables. After elimination of some variables due to weak predictive power ($r < 0.2$) or collinearity, independent variables, Z_i, are standardized and entered into a multivariate regression for the net balance,

$$b_n(t) = \beta_0 + \sum_i \beta_i Z_i(t) \,. \tag{3}$$

Variables Z_i that are retained in the final models, regression coefficients, and model performance diagnostics are summarized in Table 8. The model including Lake Louise historical station data is slightly stronger than that based solely on synoptic indices, ($R^2 = 0.60$). It includes summer temperature, T_s, winter precipitation, P_w, and three synoptic measures: summer and annual 500-mb height, Z_{500s} and Z_{500a}, along with annual flow strength, f_a (500-mb wind speed). Model B, based only on synoptic flow indices, retains the same three flow variables and has an R^2 of 0.55. This indicates that synoptic flow characterization explains 55% of the variance in the interannual mass balance variability.

Table 8. Multivariate regression coefficients for the Peyto Glacier mass balance model. See the text for an explanation of the variables. Model A includes both Lake Louise station data and NCEP/NCAR synoptic flow indices over the Canadian Rockies and Model B is confined to the latter. $|\overline{\varepsilon}|$ is the mean absolute error (L1-norm) in the annual mass balance reconstruction.

Model	β_0	β_{Ts}	β_{Pw}	β_{Z500s}	β_{Z500a}	β_{fa}	R^2	$|\overline{\varepsilon}|$ (mm)
A	−635	−202	80	−136	−199	226	0.60	302
B	−635	—	—	−321	−193	227	0.55	325

Both models have reasonable predictive skill for net mass balance (Figure 16), but variability is muted in the multivariate models. The average errors for annual mass balance reconstructions are 303 and 325 mm w.e. a^{-1} for the two models (Table 8). The model that is restricted to upper-air synoptic conditions is comparable to that employing station data. This is important for future projections, because station data are unavailable and climate models are known to be weak at predicting local conditions. In contrast, large-scale atmospheric circulation patterns predicted by climate models are expected to be relatively robust.
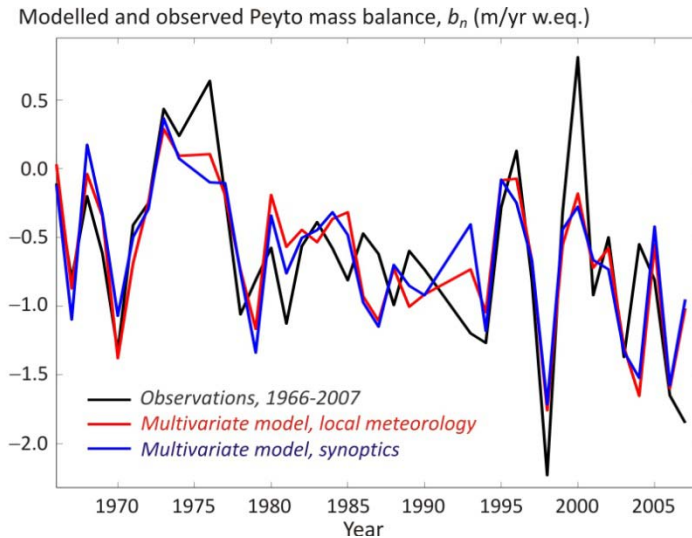
Figure 16. Observed and statistically-modelled Peyto Glacier mass balance, 1966-2007. The red line corresponds to a multivariate model based on Lake Louise summer temperatures, winter precipitation, and synoptic-scale flow indices (500-mb heights and upper air flow strength in the summer and winter). The blue line is for the multivariate regression including only the synoptic indices.

The synoptic meteorological influences on glacier mass balance can be simplified to some extent and described as the relative influence of (i) warm, southwesterly, (ii), moist, northwesterly, and (ii) cold, northerly air masses in the region. Southwesterly flow is associated with high-pressure ridging and dry subtropical air, with the jet stream north of the region. When cool air descends in weather types (ii) or (iii), the jet stream lies over or south of the region and the Rockies experience low temperatures and greater amounts of Pacific moisture. The relative frequency with which each of these synoptic setups visit the region drives the seasonal and annual weather conditions.

This is relevant because it makes Alberta's water resources particularly susceptible to climate change impacts. As Earth's climate warms, strengthening tropical circulation and more persistent El Niño conditions are pushing the jet stream northward, with subtropical air pushing into southwestern Canada with greater frequency. This is creating warmer, drier conditions that are expected to intensify in future decades. Qualitatively, one can map the climate of Idaho and Montana onto that of southwestern Canada. Quantitatively, one must turn to climate models to provide an assessment of future conditions and their implications for glacier mass balance.

5.5 Extrapolation to the Canadian Rockies

To model historical glacier mass balances on the eastern slopes of the Rockies, we assume that the year-to-year variability of mass balance at Peyto Glacier is representative of the entire region. Shea and Marshall (2007) find good coherence between regional-scale

meteorological station data for the southern Canadian Rockies, although this assumption needs to be tested in central and northern parts of our region.

Assuming linear mass balance gradients and latitudinal variations in ELA, Peyto Glacier mass balance profiles can be mapped onto regional-scale mass balance conditions. This allows us to estimate net annual mass balance as a function of altitude and latitude across the full domain, as described below. Latitudinal variations in both balance gradient and ELA are based in part on observations from Haig and Kwadacha Glaciers, near the southern and northern limits of the region.

Haig Glacier is the main outlet of a small icefield that straddles the continental divide in southern Kananaskis, Alberta. Shea et al. (2005) and Sinclair and Marshall (2009) describe the site in detail. The average ELA from 2000-2009 was 2770 m asl and the average net annual mass balance gradient, $\partial b_n / \partial z$, observed on Haig Glacier (2001-2007) was 9.8 mm w.e. m^{-1}. Average ELA and net mass balance gradients on Kwadacha Glacier for 2007-2009 were 2138 m and 6.7 mm w.e. m^{-1}. The latter is similar to the average net balance gradient on Peyto Glacier, 6.14 mm w.e. m^{-1}. We adopt 6.14 mm w.e. m^{-1} as the reference value, treating this as constant for the region.

To explore a range of sensitivity in the regional mass balance modelling, we apply the standard deviation of $\partial b_n / \partial z$ from the multiyear record at Peyto Glacier, 0.82 mm w.e. m^{-1}, giving a range of balance gradients from 5.3 to 7.0 mm w.e. m^{-1}. The balance gradient on Haig Glacier is much steeper but it covers a limited range of elevation, so it may not be regionally applicable. In the event that it is actually more representative of glaciers in the southern part of the study region, we also consider a scenario with $\partial b_n / \partial z$ = 9.8 mm w.e. m^{-1} for glaciers in the Bow and Red Deer basins.

The Haig and Kwadacha Glacier studies are short-term and these were years of strongly negative mass balance, so it is difficult to compare ELA values at these sites with the longterm record at Peyto Glacier. To estimate a latitudinal ELA gradient, we instead use the median elevation of all glaciers in the eastern slopes of the Rockies as a function of latitude (Figure 6), based on strong observed correlations between equilibrium ELA and median glacier elevation (Paterson, 1994; Kuhn, 2008). A break in the ELA-latitude relation is evident at about 55.5°N, reflecting a gap in glacier cover between the main ranges of the Canadian Rockies and the northern extension of the Rockies in B.C. We fit piece-wise linear latitudinal gradients to each region (Figure 17), with a southern gradient of −187 m°N^{-1} and a northern gradient of 118 m°N^{-1}. This positive gradient may reflect increasingly dry climate conditions at higher latitudes in the northern Rockies.

Taking these values for the ELA gradients south and north of 55.5°N, referenced to Peyto Glacier ELA, a balance gradient of 6.14 mm w.e. m^{-1}, and the glacier hypsometry, we estimate the recent volumetric mass balance of the entire region. This calculation gives an average Rockies-wide ice volume loss of 0.62 ± 0.09 km^3 a^{-1} from 2000-2007 (Table 9), equivalent to an average rate of ice volume depletion of about 1.1% a^{-1}. This represents the recent glacier contribution to streamflow, which can also be assessed for individual

catchments (Table 9). Most of this runoff takes place in the period mid-July to mid-September, when the seasonal snowpack has melted away and glacier ice is exposed.
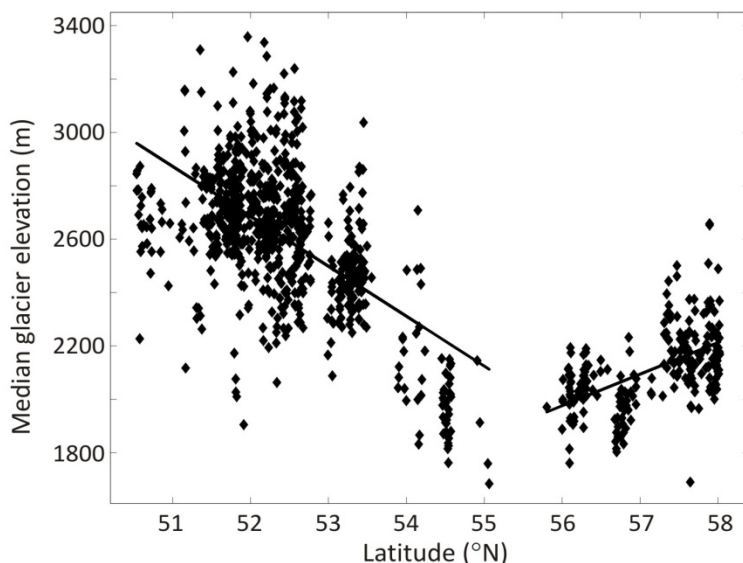
Figure 17. Median glacier elevation vs. latitude on the eastern slopes of the Canadian Rocky Mountains.

Table 9. Modelled glacier volume, rates of recent ice loss (2000-2007), and estimated timescales for future ice volume loss in each glaciated basin of the eastern slopes. Volumes are ice-equivalent. Rates of recent ice loss are also expressed as the average rate of thinning of glaciers in each catchment. Projected ice volume in 2100 is given for the reference model parameters for four cases: C1, from an extrapolation of recent rates of ice loss, without ice dynamics and geometric adjustments; C2 to C4, including glacier dynamics and geometric adjustments. C2 is based on recent (2000-2007) mass balance sustained through the 21st century. C3 and C4 are for the B1 and A1b ensemble mean future climate change scenarios (see Section 6).

| Basin | Ice volume (km^3) | Recent ice loss | | Ice volume, 2100 (km^3) | | | |
		($km^3\,a^{-1}$)	($m\,a^{-1}$)	C1	C2	C3	C4
Bow	3.0	0.081 ± 0.019*	1.35	0.0	1.0	0.2	0.1
Red Deer	0.9	0.010 ± 0.002*	0.60	0.0	0.2	0.0	—
N. Sask.	17.5	$0.226 \pm 0.030^\dagger$	0.79	0.0	7.5	1.4	0.5
Athabasca	16.7	$0.147 \pm 0.020^\dagger$	0.46	2.7	14.5	6.2	3.7
Peace	16.9	$0.156 \pm 0.021^\dagger$	0.56	2.1	9.5	3.7	1.8
Whole region	55.0	0.620 ± 0.092	0.65	4.8	32.8	11.4	6.0

* Range based on balance gradients from 6.1 to 9.8 mm w.e. m^{-1}
† Range based on balance gradients of 6.14 ± 0.82 mm w.e. m^{-1}

Uncertainty bounds on rates of volume loss in the North Saskatchewan, Athabasca, and Peace basins are based on the variability of balance gradients at Peyto Glacier. For a balance gradient of 9.8 mm m^{-1} in the Bow and Red Deer Basins, rates of 2000-2007 ice loss in these basins increase by about 50%, from 0.063 to 0.01 km^3 a^{-1} and 0.008 to 0.012 km^3 a^{-1}, respectively (Table 9). For the range of mass balance gradients explored here, estimated mass loss for the period 2000-2007 ranges from 0.53 to 0.71 km^3 a^{-1}. Given the uncertainty in current ice volume, 55 ± 15 km^3, this represents a rate of volume loss of 0.8 to 1.8 % a^{-1}.

This method cannot be used to estimate the volumetric rates of ice loss prior to the 2000s because the rapidly-declining glacier area means that the 2005 glacier snapshot is not representative. These values of discharge do, however, indicate the recent rate of depletion of the ice reservoir on the eastern slopes. Assuming a total present-day ice volume of 55 km^3, extrapolation to the future based on the average rate of ice loss in the 2000s gives an expected lifetime of 89 years. In reality, glacier hypsometry differs between basins, giving rise to different glacier response times, sensitivities to warming, and present-day mass imbalances. High-elevation niche glaciers and névé regions experience a less negative mass balance and can be expected to outlive low-elevation valley glaciers.

This simple-minded extrapolation is sobering, but it is inappropriate for several reasons: (i) climate change will accelerate the rate of ice loss relative to the historical period, (ii) continuing ice retreat upslope will mean that the glaciers will retreat to higher elevations, where they will experience less ice loss as they attempt to equilibrate with the new climate, and (iii) local climate-change feedbacks (e.g. decreasing ice albedo) and (iv) glacier dynamics will modify the climate-driven glacier response.

Recent hydrological modelling studies either neglect changes in glacier geometry (Matulla et al., 2009) or used simple methods to parameterize glacier dynamical adjustment (Stahl et al., 2008) to examine glacier response to climate change. In Section 6 we introduce simple models of glacier dynamics to account for these effects, allowing us to generate a physically-based first-order forecast for Alberta's glaciers.

5.6 Implications for Runoff

The present-day reconstructions of regional-scale mass balance and glacier retreat provide an estimate of glacier contributions to streamflow for rivers that spring from the eastern slopes of the Canadian Rockies. Glacier ice is typically exposed by mid-July in this region, with runoff from glacier melt concentrated in the period from mid-July to early September.

Monthly streamflow for the period 2000-2007 is estimated at locations of interest for each basin (Table 10). With the exception of the Athabasca River, all of these locations have regulated flows, prohibiting a direct monthly comparison. We estimate naturalized flows in the regulated basins based on the natural flows from upstream locations and tributaries, using data from Water Survey of Canada gauging stations with continuous flow measurements from 2000-2007 (Environment Canada, 2009). Monthly proportions of annual flow, relative to the downstream site of interest, are calculated for each upstream

station with natural flows. A composite of these upstream flows provides an estimate of the naturalized monthly discharge, which we scale up to provide a synthetic reconstruction of monthly natural flows at the regulated sites. The number of water survey stations and the aggregate proportion of annual yield for each catchment (i.e., the scaling factor for naturalized flow reconstructions) are given in Table 10.

Because reconstructed monthly hydrographs are based on upstream tributaries, this method does not account for losses due to evaporation, ground water effects, or the potentially different seasonal controls of the river's hydrological balance in downstream portions of the basin. Our estimates of July to September streamflow in Table 8 should therefore be treated with caution. While approximate, they do provide a perspective on glacier contributions to late-summer flow. We estimate that glacier volume losses from 2000-2007 were equivalent to 6.7% of the naturalized July to September discharge of the Bow River at Calgary, 7.4% of the North Saskatchewan River in Edmonton, and 2.0% of the Athabasca River in Fort McMurray. Glaciers contributed less than 1% to the late-summer flows in the Peace basin from 2000-2007. Glacier contributions to annual discharge range from 0.2 to 3.7% and are greatest in Calgary (2.8%) and Edmonton (3.7%).

Table 10. Average annual discharge, estimated naturalized July to September discharge, and estimated contributions from glacier volume loss (water equivalent) at sites of interest in each major glacier-fed Alberta river basin, 2000-2007. *N* and *f* indicate the number of HYDAT sites used to reconstruct the naturalized flows and the percentage of annual yield represented by these upstream sites.

Basin	Site	N	f (%)	Average yield (km^3)			% glacial	
				Q_a	Q_{JAS}	Q_g	ann	JAS
Bow	Calgary	2	45.4	2.6	1.1	0.074	2.8	6.7
Red Deer	Red Deer	3	62.2	1.4	0.5	0.009	0.6	1.8
N. Sask.	Edmonton	5	51.9	5.6	2.8	0.206	3.7	7.4
Athabasca	Ft. McMurray	1	100.0	15.9	6.6	0.134	0.8	2.0
Peace	Peace River	15	74.2	59.7	18.2	0.142	0.2	0.8

6. Climate Model Scenarios and Glacier Projections

The synoptic conditions used to estimate Peyto Glacier mass balance in Figure 16 are based on a climate model, but incorporating observational data to constrain the model; these are essentially historical reconstructions, also called climate reanalyses. In contrast, global climate models (GCMs) have also been run for the 20th century in 'free-running' mode, where the climate is freely-determined subject to prescribed atmospheric forcing from historical greenhouse gases and sulphate aerosol emissions (IPCC, 2007). Such models are not observationally constrained, so they do not reproduce the actual weather – only the mean conditions, with internal (natural) variability that is realistic but does not correspond to the timing of, for example, actual El Niño cycles or Pacific climate variability.

Model results from the Canadian GCM, CGCM3.1, are employed to test whether 20th-century synoptic variability in the GCM is representative of the Canadian Rockies and is able to produce realistic glacier mass balance fields. As shown in Figure 18, the model proves to be reasonable in this test. Figure 18b plots a comparison of the observed mass balance vs. the modelled mass balance for one realization of CGCM3.1. Five different realizations of the model are shown in Figure 18a. These are independent simulations that apply different initial conditions, allowing for a sampling of different natural variability in the simulations. Individual years cannot be compared for the reasons noted above, but the raw results indicate that the mean mass balance and the climatological trend in mass balance over the period 1966-2007 are well-reproduced. The climate model (or the multivariate regression which approximates mass balance from the CGCM synoptic fields) exhibits less interannual variability than nature, but the cumulative mass balance changes are very well-captured. This lends confidence to the potential for modelling future mass balance changes in the Canadian Rockies based on CGCM simulations.
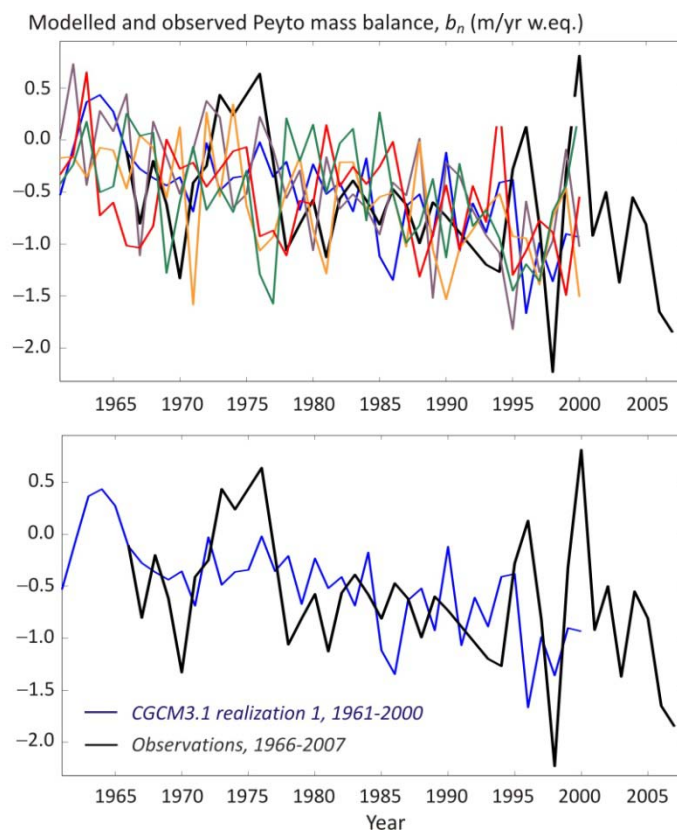
Figure 18. Observed (black) and NCEP-modelled Peyto Glacier mass balance, 1961-2007. The coloured curves indicate different climate model realizations.

Future projections are based on 21st-century simulations from the same climate model, CGCM3.1, using two standard IPCC future emissions scenarios, A1b and B1 (IPCC, 2007). These are illustrated in Figure 19. These are two middle-of-the-road scenarios that are considered to be reasonable trajectories given current population growth, development,

and energy intensity and the clear indication that the global community will not deviate from this path in the near-future. Mean annual surface air temperature in the Canadian Rockies from these two scenarios is plotted in Figure 20. The projected warming is 2-3°C, in line with global average forecasts for the 21st century.
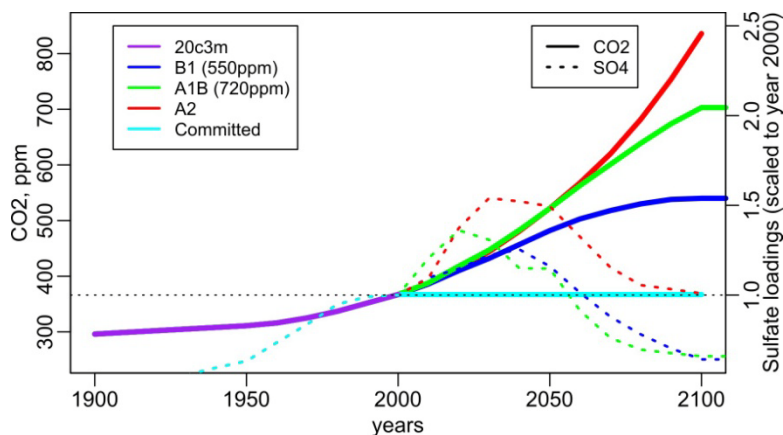
Figure 19. IPCC SRES forcings for future climate change scenarios.

To examine the likely impacts on ice cover in the Rockies, we calculate glacier mass balance using the same altitudinal and latitudinal gradients as adopted for the historical extrapolation in Section 5.5. Figure 21 plots the resulting 'theoretical' Peyto Glacier mass balance, based on the 2005 reference surface. This is the mass balance that would be expected if glacier geometry did not change. In reality, the glaciers of the Rockies will retreat upslope to areas where less melt energy is available, and the mass losses will gradually decline for a given amount of warming. It is unclear whether glacier re-equilibration will keep pace with the climate change, but glacier response times (typically several decades) and 20th-century observations suggest that this is unlikely. It is therefore impossible to predict the actual mass balance time series (hence, glacial runoff) without accounting for glacier dynamics.

To accommodate this, we include a model of glacier dynamics to allow glacier geometry to evolve in response to the cumulative mass balance forcing. We accommodate this through a simple 'lumped' model of glacier dynamics adapted from Marshall and Clarke (1999). This model uses the hypsometry and area of glaciers in a region, e.g., a climate model grid cell. Here we take the hydrological catchments as the representative regions. We divide each major river basin on the eastern slopes into 100-m elevation bands, with mean elevation h_k. The area and thickness of ice in each elevation band are denoted a_k and H_k, respectively. The model simulates the evolution of glacier geometry in response to mass balance forcing.

This approach solves the continuity equation for changes in ice thickness at each elevation level, k, as a function of local mass balance and a parameterization for the downslope transport of ice. The local conservation of mass follows

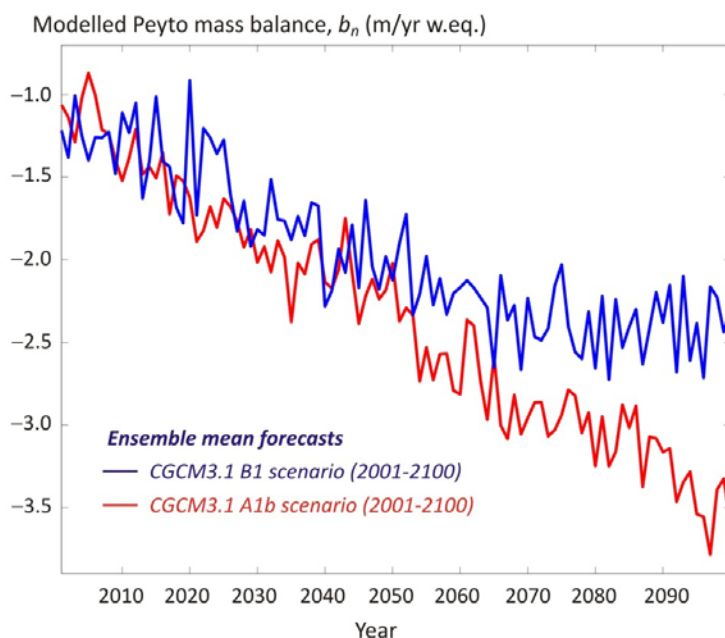$$\frac{\partial H_k}{\partial t} = -\nabla \cdot Q_k + b_k, \tag{4}$$

where Q is the ice flux (m³yr⁻¹) and b is the net annual mass balance. Ice flux is parameterized according to Glen's flow law for temperate glacier ice (Paterson, 1994) and is a strongly nonlinear function of ice thickness and surface slope,

$$Q_k = \chi \, a_k H_k^5 \, \nabla h_k^3, \tag{5}$$

where χ is a parameter that describes the ice rheology and governs the flow rate.
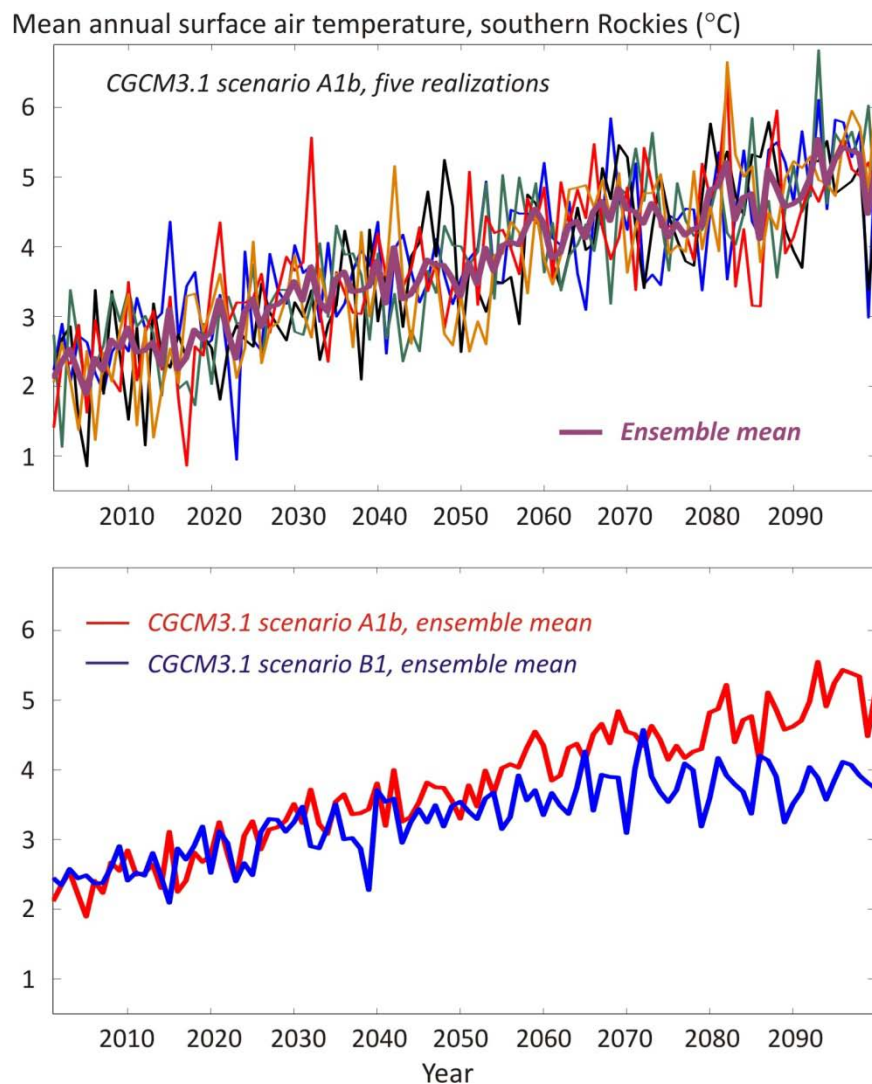
Figure 20. Forecast surface air temperature over the southern Rockies, 2001-2100, for five realizations of the A1b scenario (top panel) and the ensemble means of the A1b and B1 scenarios.

Modelled Peyto mass balance, b_n (m/yr w.eq.)

Ensemble mean forecasts
— CGCM3.1 B1 scenario (2001-2100)
— CGCM3.1 A1b scenario (2001-2100)

Figure 21. Future glacier mass balance forecasts resulting from the synoptic flow conditions in the ensemble mean CGCM climate change scenarios. Values are referenced to the 2005 glacier surface.

The ice dynamics model accounts for the downslope transport of ice from the upper elevations, so that snow does not build up at the high-elevation accumulation areas. It also allows a prognosis of glacier area and volume changes in response to changing climate. The model does not explicitly resolve individual glaciers; rather, it assumes a common mass balance and dynamical adjustment as a function of elevation for all of the glaciers within a basin.

We use χ as a tuning parameter and calibrate its value ($\chi = 1.2 \times 10^{-8} \text{ m}^{-4} \text{a}^{-1}$) from simulations that start with no ice and build up glacier cover that matches the initial (2005) ice cover, based on the target value of 55 km^3 on the eastern slopes. The simulated ice volume from a 200-year 'spinup' simulation in each catchment falls within the error bounds of the slope- and scaling-based estimates (Table 5). This initialization uses an estimate of an equilibrium mass balance state for the 20th-century (i.e. b_n= 0).

The ice dynamics model accounts for the downslope transport of ice from the upper elevations, so that snow does not build up indefinitely at the high-elevation accumulation areas. Projecting into the future, it also allows for glacier length and area changes in response to ongoing ice loss. The resulting glacier forecasts are shown in Figure 22.

The projected glacier demise is severe for this century. The top line in Figure 22a illustrates the expectations if glacier mass balance rates from 2000-2007 are maintained for the rest of the century. This is what would be expected if climate stabilized at its recent mean state. The solid black line illustrates the reference model case, with $\chi = 1.2 \times 10^{-8} \text{ m}^{-4} \text{a}^{-1}$, and the dashed black lines illustrate the sensitivity for values of χ of 0.6 and 1.8×10^{-8} m^{-4}a^{-1} ($\pm$ 50%).
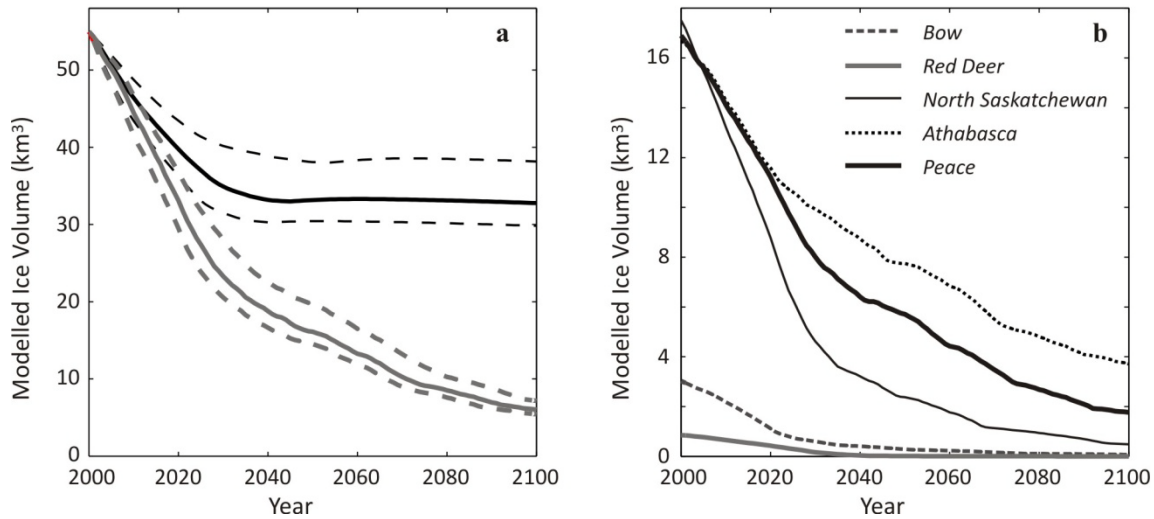
Figure 22. Ice volume forecasts for (a) all basins on the eastern slopes of the Rockies and (b) individual basins, for different mass balance scenarios combined with a model of glacier dynamical response to this forcing. (a) The upper, black lines assume that mass balance in the 21st century is fixed at the mean values for the 2000s. The lower, grey lines correspond to GCM-derived mass balance time series from the A1b climate change scenario (red line in Figure 21). Solid lines are for the reference ice dynamics model, $\chi = 1.2 \times 10^{-8}$ m^{-4} a^{-1}. The upper and lower dashed lines for each mass balance scenario are for $\chi = 0.6$ and 1.8×10^{-8} m^{-4} a^{-1}, respectively. (b) Projections for ice volume in each basin for the A1b scenario.

The model predicts several decades of ice loss, with equilibration by ca. 2040. Even with immediate stabilization of climate, 31% to 46% of the current glacier volume on the eastern slopes is lost in this 'static climate' scenario, with an estimate of 40% for the reference model. Glacier retreat differs between basins; modelled ice volume in 2100 is given in Table 5 (case C2). In all basins the geometric evolution of the glacier – the retreat to higher elevations – helps to stabilize the glaciers and extend their lifetime. Mass loss declines with time, and the cumulative loss is much less than that predicted from extrapolation of recent rates of decline. The Bow, Red Deer, North Saskatchewan, and Peace basins nevertheless see losses of 66%, 71%, 57%, and 44% of current ice volume by 2100. Athabasca basin ice masses are more resolute in this simulation, losing only 13% of present-day ice volume.

The lower curve in Figure 22a represents the more realistic forecast if the planet continues to warm, with steeper rates of ice loss and ongoing glacier retreat throughout the century (climate scenario A1b; grey lines). Relative to the case with fixed present-day climate/mass balance, rates of ice loss are greater and glacier retreat continues throughout the century, with no stabilization. Simulations are moderately sensitive to ice dynamics (dashed lines), but the future evolution is largely dictated by the climate/mass balance scenario. The total ice projected to survive the century is 11.4 and 6.0 km³ under the A1b and B1 scenarios, respectively (cases C3 and C4 in Table 5).

This amounts to a loss of 79-89% of glacier volume on the eastern slopes by 2100. About 60% of the remaining ice is in the Athabasca Basin, in the upper plateau region of the Columbia Icefield: the headwaters of the North Saskatchewan and Athabasca Rivers. High-elevation glaciers and icefields are also well-represented in the B.C. portion of the Peace River catchment in 2100. There is residual glacier cover in all basins under scenario B1, but Red Deer glaciers are eliminated under scenario A1b, while only 2% and 3% of the original glacier volume persists in the Bow and North Saskatchewan basins (Figure 22b). The ELA rises above a critical elevation threshold for glaciers in these southern basins under the future climate scenarios, while glaciers in the Peace and Athabasca basins have greater resilience.
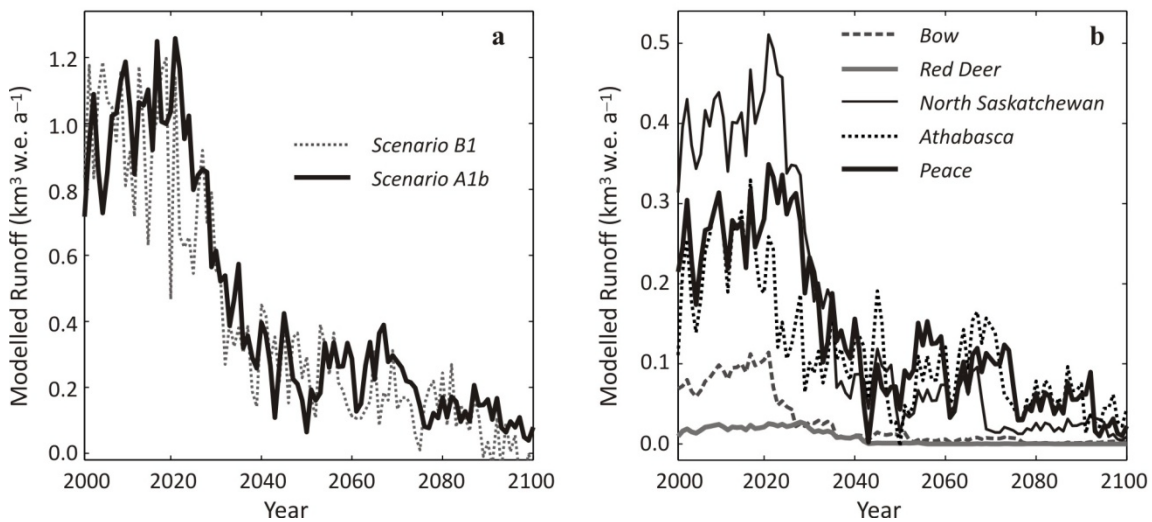
Figure 23. Modelled 21st century glacier runoff associated with the ice volume demise in Figure 22. (a) All of the eastern slopes of the Rocky Mountains and (b) for individual basins (A1b scenario).

Figure 22b plots the projected ice volume evolution for individual basins, while Figure 23 shows the corresponding glacier discharge: the expected contributions to Alberta's rivers from glacier volume loss. Modelled glacier runoff represents the release of water that has been in long-term storage in the glaciers. Melting and runoff of seasonal snow augments this glacier volume change and dominates the discharge in glacierized basins in early summer, but is not included in these calculations or discharge forecasts. Projected glacier contributions to streamflow indicate substantial declines through the 21st century, with glacier inputs decreasing from 1.1 km^3 w.e. a^{-1} in the early 2000s to less than 0.1 km^3 w.e. a^{-1} by the end of the century. These impacts on the river systems will be concentrated in late summer.

These forecasts are uncertain because we do not know the initial glacier volume well. To test the sensitivity of our forecast to estimates of the current aggregated volume, we repeated the analysis with an initial ice volume of 70 km^3 (an average ice thickness of 72

m). The projected glacier retreat follows a similar path to that of the reference case (Figure 22), with ice volume losses of more than 80%. Remaining glacier volume in 2100 is 5.5 km^3 (case A1b) and 10.8 km^3 (case B1).

Surprisingly, there is little difference from the reference model cases with an initial ice cover of 55 km^3, a discouraging result for Alberta tourism but interesting with respect to water resources impacts of glacier retreat. This result indicates that the amount of glacier ice remaining at the end of the century is largely insensitive to the present amount of ice, although the amount of glacier meltwater contributing to Alberta's rivers over the next 100 years differs in these two simulations. An initial ice volume of 70 km^3 gives roughly 30% more total glacier discharge relative to the 55 km^3 used in our climate simulations (Figure 23), and glacier contributions to streamflow continue longer into the century.

This lack of sensitivity to initial conditions is due to the over-riding climatic control of glacier retreat. The ELA in the main glacierized region of the Rockies rises to over 3000 m by the end of the century in these simulations, meaning that most of the glacier area in the region (cf. Figure 2) lies in the ablation zone, and ample melt energy exists to down-waste 57 or 72 m of ice over this century. Irrespective of initial conditions, most of the remaining glaciers in 2100 lie in high-elevation plateau environments such as the Columbia Icefields, which feed the North Saskatchewan and Athabasca Rivers. High-elevation glaciers also endure in the Peace River catchment.

Final ice volumes are also insensitive to the choice of ice transport coefficient, χ, although this affects the rate of ice-dynamic adjustment and therefore the rate of glacier decline in the early parts of this century. Higher values of χ – increased ice discharge – hasten the glacier volume loss by transporting more ice to the lower elevations, where it melts more readily. This implicitly includes the effects of glacier sliding, which increases transport rates. Holding χ constant is equivalent to an assumption that the importance of glacier sliding will not change this century. Other changes in glacier dynamics, as a function of ice thickness and surface slope, are explicit in the ice-flux parameterization, Eq. (5).

There is little constraint on χ, but the lumped treatment of each river basin means that this free parameter should not be interpreted in terms of the dynamics of individual glaciers; it is a bulk treatment of downslope ice transport on a basin scale. Many improvements could be made to this approach. For instance, glaciers within a basin could be grouped by aspect (e.g., north vs. south-facing) or by glacier type (e.g., cirque, valley, icefield), with their mass balance and dynamics treated differently. In principle, individual glaciers could also be modelled using this simple dynamical parameterization and all of the glaciers in the region could be explicitly modelled.

7. Summary and Recommendations

The focus of this study is to make an accurate estimate of ice volume given current knowledge of glaciers in the Rockies. We estimate this to be 55 ± 15 km³ for all of the glaciers in the eastern slopes, with 47 ± 15 km³ in Alberta and the remainder in the eastward-draining ice masses of the Peace River Basin in B.C. More than 75% of Alberta's ice is contained in the headwaters of the North Saskatchewan and Athabasca Rivers, where the largest icefields are clustered.

The lack of glacier thickness (volume) data in the Canadian Rockies is very limiting. Without this data volume estimates have a high degree of error and models of ice dynamics cannot be expected to give realistic, detailed predictions of glacier response to ongoing climate change. Ice thickness measurements through surface and airborne ice radar studies would be extremely valuable to improve on these uncertainties. Ice thickness studies across a suite of glacier size classes and glacier types are recommended. In particular, volume-area scaling relationships should be developed and tested for cirque glaciers and plateau icefields in the Rockies. More data from small- and intermediate-sized valley glaciers would help to reveal whether Athabasca Glacier is anomalously thick or if it is genuinely representative of the Canadian Rockies. Ice-thickness data from the Haig Glacier suggests that the latter may be true, but more studies are needed. Well-designed airborne radar ice-thickness mapping surveys would help to resolve this.

Notwithstanding the challenge of predicting an accurate volume estimate from the current data, more could be done to examine the consistency of the estimates presented here. In particular, alternatives to volume-area scaling could be explored, such as that of Farinotti et al. (2009), which involves more detailed terrain characterization. Clarke et al. (2009) introduce an inverse method to approximate subglacial topography, based on analysis of the geometry of the current glacier cover and the surrounding terrain. Assumptions about glacier rheology and stress regime allow estimates of ice thickness to be estimated from the surface slope. Clarke et al. (2009) take this further and employ a neural network analysis that incorporates information from the surrounding terrain. This methodology is non-trivial but could be applied to the Rockies for an additional or alternative estimate of the present-day ice volume.

The volume estimate should be seen as a starting point for studies that include monitoring of volume and runoff changes in future years and decades. Studies of historical glacier volume loss have already been undertaken. Through the use of Shuttle Radar Topography Mission (SRTM) DEM data and archived DEMs from aerial imagery, glacier surface elevation changes can be found. The change in volume is then calculated by multiplying the difference in the surface height by surface area. This approach has been used in several mountain regions, including Alaska and B.C. (Schiefer et al., 2007), and it provides a direct measure of glacier runoff. Ongoing monitoring of this type should be undertaken through LIDAR surveys (airborne laser profiling) of key icefields and glaciers, to provide volume-change estimates that can be tested against discharge records and provide empirical insight into regional trends.

Working from the area, hypsometry, and estimated volume of glacier ice in the year 2005, we apply a simple model of glacier mass balance to the eastern slopes of the Rocky Mountains and estimate recent and future contributions to streamflow associated with continued glacier retreat. This model is based on net mass balance gradients on Peyto, Haig, and Kwadacha Glaciers, the relation between historical mass balance variations and synoptic meteorological conditions at Peyto, and latitudinal ELA gradients across the region. Based on the regional mass balance model, we estimate recent (2000-2007) glacier runoff from the eastern slopes to be 0.62 ± 0.09 km^{3}a^{-1}, equivalent to 3-4% of mean annual discharge and 7-8% of late summer (July to September) runoff in the North Saskatchewan and Bow Rivers in Edmonton and Calgary.

Future projections of the glacier cover on the eastern slopes, including a simple model of glacier dynamics, provide estimates of how glacier volume and runoff may change in the coming decades. If climate stabilizes such that mass balance rates like those of the 2000s persist through the 21st century, about 40% of the glacier ice in the Rocky Mountains will disappear this century. If climate change continues as per the projections from the A1b or B1 climate scenarios, we estimate an 80 to 90% decrease in glacier volume by the end of the century.

Our models of regional glacier mass balance and glacier dynamics are simple, so we consider this to be a first-order, initial forecast for the 21st-century evolution of glaciers in the Rockies. Our model neglects the detailed topographic situation, climatology, and controls of mass balance for individual glaciers. More sophisticated, spatially-explicit models of glacier mass balance and ice dynamics should be developed and applied for improved, physically-based forecasts. Such models exist for individual glaciers (e.g. Schneeberger et al., 2001), but there are significant challenges to simulating glacier evolution on a 'watershed' or 'mountain range' scale; climate and mass balance scenarios need to be realized at a resolution of 100s of metres, and a complete model of glacier dynamics requires detailed knowledge of the underlying bedrock topography. We lack the data for a full treatment, but more sophisticated, physically-based models could be applied for portions of a basin to test and evaluate our projections.

Acknowledgements

References

Bahr, D.B., Meier, M.F. and S.D. Peckham, 1997. The physical basis of glacier volume-area scaling. *Journal of Geophysical Research*, 102, 20,355-20,362.

Barnett T.P., J.C. Adam and D.P. Lettenmaier, 2005. Potential impacts of a warming climate on water availability in snow-dominated regions. *Nature* 438: 303-309.

Bitz, C. and D. Battisti. 1999. Interannual to decadal variability in climate and the glacier mass balance in Washington, Western Canada and Alaska. J. Climate, 12, 3181-3196.

Bolch, T., B. Menounos, and R. Wheate. 2010. Landsat-based inventory of glaciers in western Canada, 1985-2005. *Remote Sensing of Environment* 114: 127-137.

Chen, J. and A. Ohmura, 1990. Estimation of alpine glacier water resources and their change since the 1870s. Hydrology of Mountainous Regions. I-Hydrological Measurements of the Water Cycle. *IAHS Publication*, 193, 127-135.

Clarke, G.K.C., Berthier, E., Schoof, C.G. and A.H. Jarosch, 2009. Neural networks applied to estimating subglacial topography and glacier volume. *Journal of Climate*, 22, 2146-2160.

Cogley, J.G., 2009. A more complete version of the World Glacier Inventory. *Annals of Glaciology*, 50(53), 8-14.

Comeau, L.E.L., A. Pietroniro and M.N. Demuth, 2009. Glacier contribution to the North and South Saskatchewan Rivers. *Hydrol. Process.* 23, 2640-2653.

Demuth, M.N. and R. Keller, 2006. An assessment of the mass balance of Peyto Glacier (1966-1995) and its relation to recent and past-century climatic variability. In *Peyto Glacier: One Century of Science*, Demuth, M.N., D.S. Munro, and G.J. Young (Eds.), National Hydrology Research Institute, Science Report, 8, 83-132.

Demuth, M., V. Pinard, A. Pietroniro, B. Luckman, C. Hopkinson, P. Dornes, and L. Comeau, 2008. Recent and past-century variations in the glacier resources of the Canadian Rocky Mountains: Nelson River system. In *Mountain glaciers and climate changes of the last century*, Bonardi, L. (Ed.), *Terra Glacialis*, 27-52.

de Woul, M., R. Hock, M. Braun, T. Thorsteinsson, T. J hannesson, and S. Halldorsdottir, 2006. Firn layer impact on glacial runoff – A case study at Hofsjökull, Iceland. *Hydrological Processes*, 20, 2171-2185.

Environment Canada, 2009. Water Survey of Canada HYDAT data. Accessed from: http://www.wsc.ec.gc.ca/products.

Environment Canada, 2010a. Water Survey of Canada HYDAT data. Accessed from: http://www.wsc.ec.gc.ca/products.

Environment Canada, 2010b. National climate data and information archive. Accessed from: http://www.climate.weatheroffice.gc.ca/ClimateData.

Farinotti, D., M. Huss, A. Bauder, M. Funk, and M. Truffer. 2009. A method to estimate ice volume and ice thickness distribution of alpine glaciers. *Journal of Glaciology* 55 (191): 422-430.

Fountain, A.G. and W.V. Tangborn, 1985. The effect of glaciers on streamflow variations. *Water Resources Research*, 21 (4), 579-586.

Fountain, A.G. and J.S. Walder, 1998. Water flow through temperate glaciers. *Reviews of Geophysics*, 36 (3), 299-328.

Gordon, S., M. Sharp, B. Hubbard, C. Smart, B. Ketterling and I. Willis, 1998. Seasonal reorganisation of subglacial drainage inferred from measurements in boreholes. *Hydrological Processes*, 12, 105-133.

Hannah, D.M. and A.M. Gurnell, 2001. A conceptual, linear reservoir runoff model to investigate melt season changes in cirque glacier hydrology. *Journal of Hydrology*, 246 (1), 123-141.

Hock, R. and R. LeB. Hooke, 1993. Evolution of the internal drainage system in the lower part of Storglaciaren, Sweden. *Geological Society of America Bulletin*, 105, 537-546.

Hock, R., P. Jansson and L.N. Braun, 2005. Modelling the response of mountain glacier discharge to climate warming. In *Global Change and Mountain Regions*, (U.M. Huber, H.K.M. Bugmann and M.A. Reasoner, Eds.), *Advances in Global Change Research*, 23 (2), Springer, The Netherlands, pp. 243-252.

Hopkinson, C. and G.J. Young, 1998. The effect of glacier wastage on the flow of the Bow River at Banff, Alberta. *Hydrological Processes*, 12, 1745-1762.

Jansson, P., R. Hock and T. Schneider, 2002. The concept of glacier storage: A review. *Journal of Hydrology*

Kaab, A., C. Huggel, F. Paul, R. Wessels, B. Raup, H. Kieffer and J. Kargel, 2002. Glacier monitoring from ASTER imagery: Accuracy and applications. Proceedings of EARSeL-LISSIG-Workshop Observing our Cryosphere from Space, Bern, 43-53.

Kuhn, M., Abermann, J., Bacher, M., and Olefs, M. 2008. The transfer of mass-balance profiles to unmeasured glaciers. *Annals of Glaciology* 50(50):185 – 190.

Letréguilly, A. 1988. Relation between the mass balance of western Canadian mountain glaciers and meteorological data. *Journal of Glaciology* 34: 11-17.

Lewandowski, W. and M. Zgorzelski, 2004. Wall-sided glaciers. *Miscellanea Geographica*, 11, 75-80.

Luckman, B. and T. Kavanagh, 2000. Impact of climate fluctuations on mountain environments in the Canadian Rockies. *Ambrio*, 29, 371-380.

Mair, D., I. Willis, B. Hubbard, U. Fischer, P. Nienow and A. Hubbard, 2003. Hydrological controls on patterns of surface, internal and basal velocities during three "spring events": Haut Glacier d'Arolla, Switzerland. *Journal of Glaciology*, 49, 555-567.

Marshall, S.J. and G.K.C. Clarke. 1999. Ice sheet nucleation: Subgrid hypsometric parameterization of mass balance in an ice sheet model. *Climate Dynamics* 15: 533-550.

Marshall, S.J., E.C. White, M.N. Demuth, T. Bolch, R. Wheate, B. Menounos, M. Beedle and J.M. Shea, in press. Glacier water resources on the eastern slopes of the Canadian Rocky Mountains. *Canadian Water Resources Journal.*

Matulla, C., E. Watson, S. Wagner, and W. Schöner Metulla, 2009. Downscaled GCM projections of winter and summer mass balance for Peyto Glacier, Alberta, Canada (2000-2100) from ensemble simulations with ECHAM5-MPIOM. *International Journal of Climatology* 29 (11), 1550-1559.

Meier, M.F. and D.B. Bahr, 1996. Counting glaciers: Use of scaling methods to estimate the number and size distribution of the glaciers of the world. Glaciers, Ice Sheets and Volcanoes: A tribute to Mark F. Meier (ed S.C. Colbeck) 1-120. Special report, 96-27. Cold Regions Research and Engineering Laboratory, Hanover NH.

Meier, M.F. and A.S. Post, 1962. Recent variations in mass net budgets of glaciers in western North America, in Variations of the regime of existing glaciers. International Union of Geodesy and Geophysics, *International Association of Scientific Hydrology*, 58, 63-77.

Meier, M.F., M.B. Dyurgerov, U.K. Rick, S. O'Neel, W.T. Pfeffer, R.S. Anderson, S.P. Anderson and A. F. Glazovsky, 2007. Glaciers dominate eustatic sea-level rise in the 21st century. *Science*, 317, 1064-1067.

Nienow, P.W., M.J. Sharp and I.C. Willis, 1998. Seasonal changes in the morphology of the subglacial drainage system, Haut Glacier d'Arolla, Switzerland. *Earth Surface Processes and Landforms*, 23, 825-843.

Oerlemans, J., Anderson, B., Hubbard, A., Huybrechts, Ph., Johannesson, T., Knap, W.H., Schmeits, M., Stroeven, A. P., van de Wal, R. S. W., Wallinga, J. and Z. Zuo, 1998. Modelling the response of glaciers to climate warming. *Climate Dynamics*, 14, 267-274.

Oerter, H., D. Baker, H. Moser, and O. Rienwarth, 1981. Glacial-hydrological investigations at the Vernagtferner Glacier as a basis for a discharge model. *Nordic Hydrology*, 12, 335-348.

Ommanney, C.S.L., 2009. Canada and the World Glacier Inventory. *Annals of Glaciology*, 50 (53), 5-10.

Paterson, W.S.B., 1964. Variations in velocity of Athabasca Glacier with time. *Journal of Glaciology*, 5 (39), 277-285.

Paul, F., A. Kääb, M. Maisch, T. Kellenberger and W. Haeberli, 2002. The new remote sensing derived Swiss Glacer inventory: I. Methods. *Annals of Glaciology*, 34, 355-361.

Paul, F., A. Kääb, M. Maisch, T. Kellenberger and W. Haeberli. 2004. Rapid disintegration of Alpine glaciers observed with satellite data. *Geophysical Research Letters* 31: L21402, doi:10.1029/2004GL020816.

Radic, V., R. Hock and J. Oerlemans, 2008. Analysis of scaling methods in derving future volume evolutions of valley glaciers. *Journal of Glaciology*, 54, 601-612.

Schiefer, E., B. Menounos and R. Wheate, 2007. Recent volume loss of British Columbian glaciers. *Geophysical Research Letters*, 34, 1-6

Shea, J.M. and S.J. Marshall, 2007. Synoptic controls on regional precipitation and glacier mass balance in the Canadian Rockies. *Int. Journal of Climatology*, 27 (2), 233-247.

Shea, J.M., S.J. Marshall and J.M. Livingston, 2004. Glacier distributions and climate in the Canadian Rockies. *Arctic, Antarctic and Alpine Research*, 36, 272-279.

Shea, J. M., F.S. Anslow, and S.J. Marshall, 2005. Hydrometeorological relationships on the Haig Glacier, Alberta, Canada. *Annals of Glaciology*, 40, 52-60.

Sinclair, K.E. and S.J. Marshall, 2009. The impact of vapour trajectory on the isotope signal of Canadian Rocky Mountain snowpacks. *Journal of Glaciology* 55 (191), 485-498.

Stahl, K., R.D. Moore, J.M. Shea, D.G. Hutchinson and A. Cannon, 2008. Coupled modelling of glacier and streamflow response to future climate scenarios. *Water Resources Research* 44, W02422, doi:10.1029/2007WR005956.

Surazakov, A. B. and V. B. Aizen. 2006. Estimating volume change of mountain glaciers using SRTM and map-based topographic data. *IEEE Transactions on Geoscience and Remote Sensing*, 44, 2991-2995.

Van de Wal, R.S.W. and M. Wild, 2001. Modelling the response of glaciers to climate change by applying volume-area scaling in combination with a high resolution GCM. *Climate Dynamics*, 18, 359-366.

Willis, I., N. Arnold and B. Brock, 2002. Effect of snowpack removal on energy balance, melt and runoff in a small supraglacial catchment. *Hydrological Processes*, 16, 2721-2749.

Glossary of Terms

A number of glaciological terms appear throughout this report. Following are conventional definitions for the most common terms. Paterson's (1994) *The Physics of Glaciers* provides further elaboration of these terms. The list of definitions below is far from comprehensive; a more complete glossary can be found at http://nsidc.org/cryosphere/.

Ablation. Snow and ice removed from a glacier via meltwater runoff, sublimation, wind scour, or calving (mechanical fracturing and separation).

Ablation Zone. The area of a glacier where annual ablation exceeds annual accumulation, giving net loss of snow and ice.

Accumulation. Snow and ice added to a glacier via snowfall, deposition, rainfall that freezes on/in the glacier, refrozen meltwater, wind deposition, and avalanching.

Accumulation Zone. The area of a glacier where annual accumulation exceeds annual ablation, giving net accumulation.

Accumulation Area Ratio (AAR). The fractional area of a glacier's accumulation zone at the end of the summer melt season. (AAR = Accumulation zone area / Glacier area).

Englacial. Within the body of a glacier.

Equilibrium Line Altitude (ELA). The elevation at which snow accumulation equals snow ablation (i.e., the elevation of the transient snow line) at the end of the summer.

Firn. Multiyear snow that is in transition from meteoric snowfall to glacier ice. Typical firn densities are 550-900 kg/m^3.

Glacier. A perennial ice mass formed from accumulated snowfall, which transforms to crystalline ice after burial and compression. The transformation from snow to ice takes several years for mountain glaciers. To be considered a viable glacier (vs. a snow or ice patch), the ice mass needs to be sufficiently large (0.1 km^2 or more) and dynamic – there needs to be evidence of ice motion.

    Ice Cap. A dome of glacier ice that overwhelms the local bedrock topography, with the ice flow direction governed by the shape of the ice cap itself.

    Icefield. A sheet of glacier ice in an alpine environment in which the ice is not thick enough to overwhelm the local bedrock topography, but is draped over and around it; glacier flow directions in an icefield are dictated by the bed topography.

    Valley Glacier. A glacier bounded by lateral rock walls and occupying an alpine valley. These can stand alone or they can be outlets for icefields and ice caps.

    Cirque Glacier. A glacier nested within a bowl-shaped depression eroded into the wall of a mountain.

Hanging Glacier. A glacier that terminates on a cliff face but is unsupported or unbounded by valley walls.

Glacier Ice. Polycrystalline ice formed from snow metamorphism, with a density of 900 to 920 kg/m^3.

Glacier Mass Balance. The overall gain or loss of mass for a glacier over a specified time interval, typically one glaciological year: net annual accumulation less net annual ablation. This can be expressed as a rate of change of mass (kg yr^{-1}), ice volume (km^3 ice yr^{-1}), or water-equivalent volume (km^3 yr^{-1}). It is also common to express this as the area-averaged rate of change or the *specific mass balance rate*, with units of kg m^{-2} yr^{-1} or m w.eq. yr^{-1}.

Glaciological Year. For Northern Hemisphere mountain glaciers such as those of Alberta, the glaciological year is a 12-month period beginning in September (when seasonal snow accumulation begins) and ending in August (the end of the melt season).

Proglacial. The environment adjacent to a glacier, also commonly referred to as the glacier *forefield*. For most contemporary glaciers, the proglacial environment is the recently-deglaciated region where vegetation has yet to take hold.

Subglacial. Below a glacier, at the interface with the underlying bedrock or sediments.

Supraglacial. On the surface of a glacier.

Surface Mass Balance. The mass balance at the glacier surface (the atmosphere-glacier interface), primarily associated with net annual snow accumulation less net annual melting. This is often referred to as the glacier's "mass balance", but strictly speaking the latter also includes the gain and loss of ice in englacial, subglacial, and ice-marginal environments (i.e. associated with calving).

Transient Snow Line. The transition zone between bare glacier ice and seasonal snow cover on a glacier surface. The transient snow line moves upward through the summer melt season as the seasonal snow cover melts.

Water Equivalence (w.eq.). Snow and ice have densities less than that of water, so for water resources applications it is helpful to express a volume of snow or ice as 'water-equivalence', e.g., a 2-m snowpack with a density of 500 kg/m^3 is equivalent to 1 m w.eq.